Computer-Assisted Frameworks for Classification of Liver, Breast and Blood Neoplasias via Neural Networks: a Survey based on Medical Images

(Article begins on next page)

17 May 2024

Computer-Assisted Frameworks for Classification of Liver, Breast and Blood Neoplasias via Neural Networks: a Survey based on Medical Images

Antonio Brunetti[a], Leonarda Carnimeo[a], Gianpaolo Francesco Trotta[b],
Vitoantonio Bevilacqua[a]

[a]*Department of Electrical and Information Engineering (DEI),
Polytechnic University of Bari. Via Orabona 4, 70126 - Bari, Italy.*
[b]*Department of Mechanics, Mathematics and Management Engineering (DMMM),
Polytechnic University of Bari. Via Orabona 4, 70126 - Bari, Italy.*

Abstract

Computer Aided Decision (CAD) systems can support physicians in classifying different kinds of breast cancer, liver cancer and blood tumors revealed also by images acquired via Computer Tomography, Magnetic Resonance, and Blood Smear systems. On this proposal, this survey is focused on papers dealing with the description of existing CAD frameworks for the classification of the three mentioned diseases by detailing existing CAD workflows based on identical steps for these mentioned tumors. In detail, after an accurate image acquisition, the fundamental steps carried out by a CAD framework can be listed as image segmentation, feature extraction and classification. In particular, in this work specific CAD frameworks are considered, where the task of feature extraction is performed both by using traditional handcraft strategies and a Convolutional Neural Network-based innovative methodology. In this latter case, the final supervised pattern classification is based on neural/non-neural machine learning methods. The cited methodology is focused by sharing and reviewing an amount of specific works. Then, the performances of three selected case studies, designed to show how final outcomes can vary on the basis of different choices in each step of the adopted workflow, are carefully reported. More in detail, these case studies concern with breast images acquired from Tomosynthesis and Magnetic Resonance, hepatocellular carcinoma images acquired by Computer Tomography enhanced by a triphasic protocol with a contrast medium, and peripheral blood smear images for cellular blood tumors and are used to compare their performances

from a quantitative point of view.

1. Introduction

In the last decades, the amount of deaths due to cancer has significantly increased, overcoming the number of deaths caused by heart attacks and stroke, as emphasized in the reports of the World Health Organization [1]. More in detail, in several industrialized countries there are determined neoplasias with a high incidence, but an early non-invasive diagnosis and staging can luckily prevent bad prognosis in some of them.

The three tumour forms considered in this survey have been evaluated among the top ten in the world for estimated number of deaths [2]. This can be well noticed in Fig 1, where in 2012 the amount of deaths for liver tumour has been estimated at the second position all over the world; the amount of deaths for breast tumour is at the fifth position all over the world, whereas the number of deaths for leukemia has the tenth value in the world in the same figure.

It can be noticed that the same three malignant forms reveal among the top ten in Italy, but they seem globally to present a more socially impacting situation [3]. In fact, in 2012 the amount of deaths for breast tumour has been the third as reported in Fig. 2, the number of deaths for liver tumour has been estimated at the sixth position and the amount of deaths for leukemia is at the eight place.

On this proposal, a first basic concept has to be pointed out, that is to say, *Image Diagnostics* is a great choice for its high ability to stage the course of each of the considered three diseases, without being excessively invasive. In detail:

- for the breast cancer: (i) in tomosynthesis it is important to note that doses of ionizing radiation far below those released in the conventional CT are released; (ii) in magnetic resonance ionizing radiation is not considered;

- for hepatocellular carcinoma: in CT with contrast medium, the contrast medium is very characteristic and therefore able to reduce the frequency of subsequent examinations;
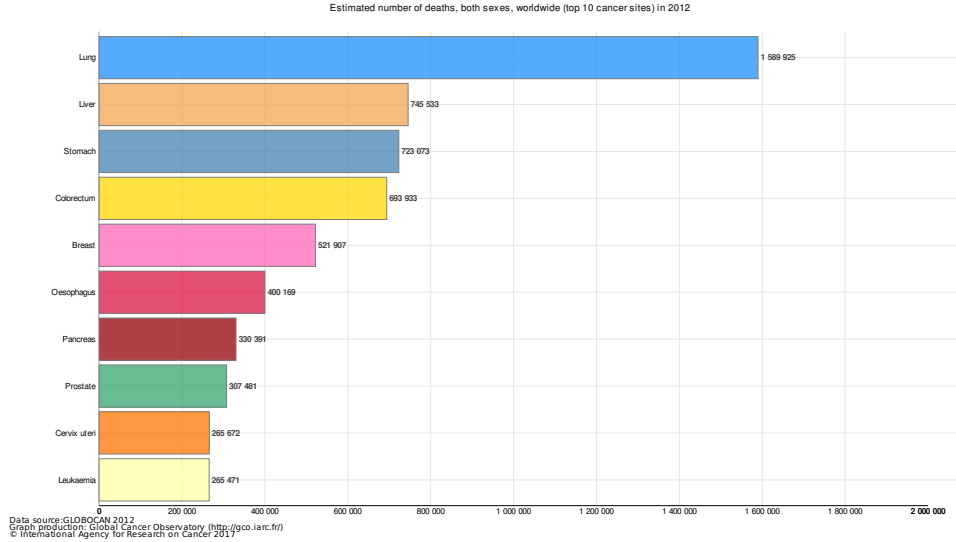
Figure 1: Estimated number of deaths caused by tumours worldwide in 2012 [2]

- for leukemia: in the peripheral strips, the method of capturing the images is absolutely non-invasive because it requires only a blood draw.

Medical imaging is a fundamental methodology for representing the internal organs of the human body, allowing a non-invasive and accurate diagnosis of several diseases, including neoplasias [4]. On this proposal, it should be precised that there are different imaging techniques able to highlight the characteristics of the human body, on the basis of the sensors used to acquire information and produce the representation of each internal organ [5]. Moreover, beside the diagnostic capabilities, medical imaging is also crucial for staging and monitoring the clinical course of each disease under investigation [6, 7, 8].

All the previously described advantages led the scientific community to study and develop a large number of automatic systems, based on medical imaging, with the aim of supporting physicians in diagnosing, staging and monitoring different pathologies. On this proposal, a large number of works focused on Computer Aided Diagnosis (CAD) systems can be found in the literature, and Fig. 3 shows the number of publications per year from 2006 to 2016 in the field of medical imaging, that is, how CAD systems have become very popular in literature [9]. In [9] authors discuss how CAD systems can
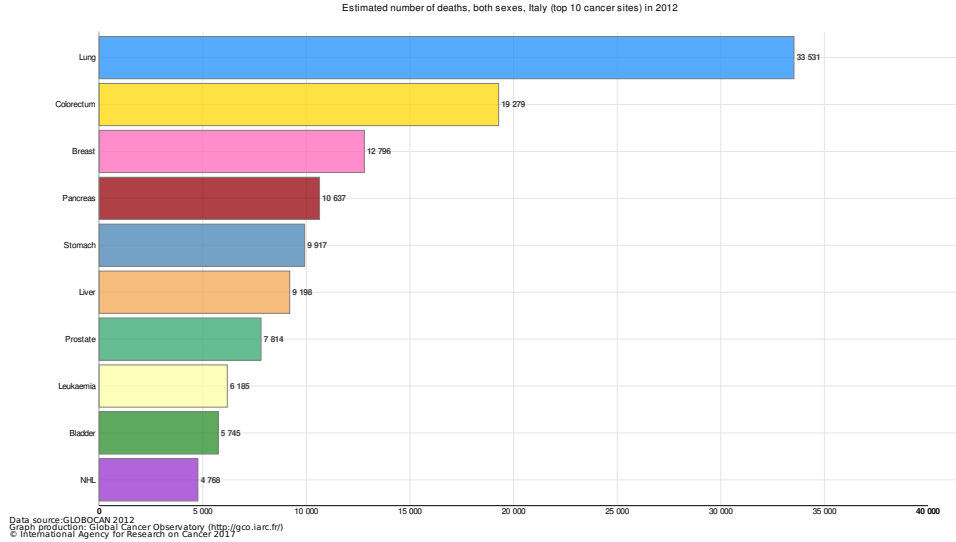
3

Figure 2: Estimated number of deaths caused by tumours in Italy in 2012 [3]

support clinicians in diagnosing, offering a cheap and suitable alternative to a data double reading intended as a mean for reducing errors.

In this work, a survey on computer-assisted frameworks for the segmentation and the automatic classification of images of tumours is presented. Existing CAD systems are herein analysed by considering the workflow on which these automatic systems are based, starting from the acquisition methods, progressing to the image processing algorithms and finally to the classification methodology.

In particular, the topic of this survey will be focused on three typologies of cancer, which are: breast cancer, hepatocellular carcinoma and blood tumour. The main motivation of this choice lies in the fact that, due to medical imaging, the detection and diagnosis of diseases can reach high levels of accuracy for these kinds of neoplasias, still preserving the non-invasiveness of the acquisition protocol.

The second main concept which leads the survey is based on the observation that CAD frameworks with the best performance are those CADs that plan feature extractions (handcrafted or via CNN) and classification approaches based on supervised machine learning techniques.

This survey is organized as follow: an introduction shows common aspects of the three considered malignant tumour forms, among which the
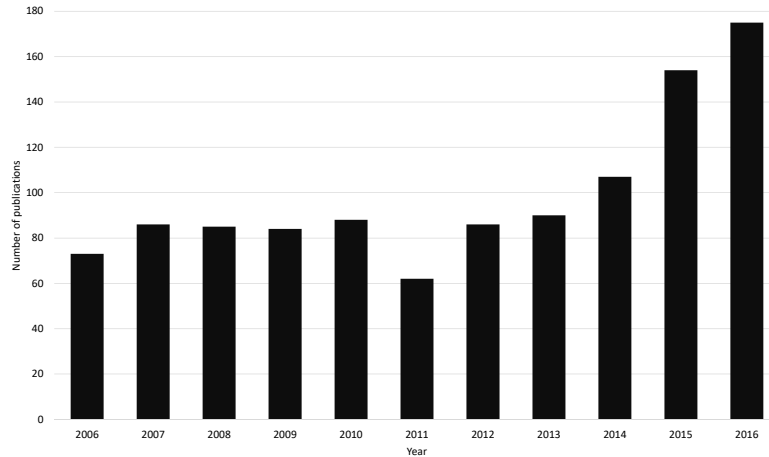
4

Figure 3: Number of publications per year from 2006 to 2016. Topic: Computer Aided Diagnosis & Medical Imaging. Indexes: SCI-EXPANDED, SSCI, A&HCI, CPCI-S, CPCI-SSH, ESCI.

potentiality of early diagnoses, and the importance of staging. Moreover, the possibility of using not too invasive techniques is explored, as well as, the need of doing both a continuous monitoring and a periodic one and if conditions of familiarity exist, or what else.

It will be shown that CAD frameworks for these diseases are similarly classified by following the same data processing chain both in literature and in considered published applicative cases.

In Section 2 the typical workflow needed to perform an automatic classification of the different tumours is introduced, which is shared by the most of existing CAD systems explored in the survey. In Section 3, 4, and 5 of this survey the existing CAD systems will be detailed, focusing on the three considered cancers. Finally, in Section 6 the examined frameworks adopted in the analysed literature will be discussed.

2. Standard Workflow of Computer Assisted Frameworks

All CAD systems based on medical imaging share an analogous detailed workflow, which enables to classify a particular tumour starting from the
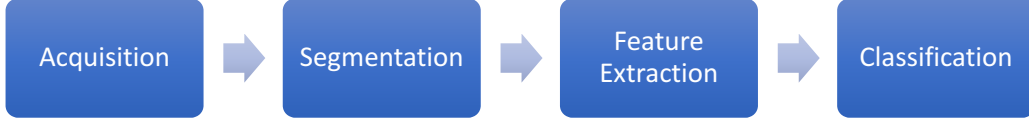
Figure 4: Traditional workflow implemented by CAD systems.

acquisition procedure, independently from the disease under investigation. The flowchart depicted in Fig. 4 shows the essential steps needed to perform the classification task. In detail, the pipeline is usually composed by four phases as follows: (1) Image Acquisition, (2) Image Segmentation, (3) Feature Extraction, (4) Classification.

2.1. Image Acquisition

In this paragraph, image acquisition technologies, based on tomography, magnetic resonance imaging and hematochemic, will be in general discussed and the available bibliography will be accurately reviewed. Screening protocols and techniques will be briefly introduced to enrich information, i.e., contrast media, periodicity of acquisitions, etc.

On this proposal, during the last decades, thanks to the increasing availability of computational resources, new medical imaging technologies have been developed and commercialized. Computed tomography, MRI imaging, Digital Subtraction Angiography, Doppler ultrasound-imaging, and various imaging techniques based on nuclear emission, such as Positron Emission Tomography (PET) or Single-Photon Emission Computed Tomography (SPECT) have all been valuable additions to the radiologist's spectrum of imaging tools toward an ever more reliable detection and diagnosis of diseases [10, 11, 12, 13, 14]. It can be noted that the optimal acquisition device can be selected on the basis of the objective of investigation, in order to highlight specific areas of the human body.

In particular, although image capture techniques may be subdivided according to various criteria, as, for example, depending on the physical principle on which the respective detectors or sensors are based, this survey will focus only on the characteristics, which lead to the less invasive methods for detecting each neoplasia and, at the same time, more targeted to acquire as much information as possible on the basis of the most modern strategies.

More in detail, concerning with breast cancer, only the tomosynthesis will be taken into consideration, which, compared to the conventional CT,

provides for a lower release of ionizing radiation, together with magnetic resonance imaging that does not exhibit any ionizing radiation. Moreover, CADs for detecting breast tumours can support in differentiating benign from malignant forms with a high accuracy and a short training time. As a consequence, they are clinically very useful to reduce the number of biopsies of benign lesions and can offer a second reading to assist inexperienced physicians in avoiding misdiagnosis.

Concerning with liver cancer, while taking into consideration the traditional CT, the most modern triphasic techniques with contrast medium will be particularly discussed, as they allow to be given a more accurate ability to recognize HCC lesions and stage the evolution of lesions more accurately for an analogous dose, avoiding to repeat CT examinations very frequently.

Dealing with leukemia, however, minimal invasive strategies such as those related to simple blood sampling supported by imaging for more accurate classification of leukocyte forms and their counting will be considered.

2.2. Image Segmentation

In this paragraph, edge-based or feature-based segmentation techniques will be globally discussed, together with pre-processing phases, such as object recognition and ROI recognition. In particular, segmentation is a crucial task in medical image processing. The accuracy of segmentation can directly affect other post-processing tasks, such as image analysis and feature extraction [15].

After the acquisition of images, a processing phase is needed for the improvement of their quality and an eventual removal of artifacts [16]. This is a crucial step in order to reach an optimal result in subsequent phases, since the outputs of this phase affect the performance of the whole workflow. As far as medical imaging is concerned, in literature there is a huge number of useful algorithms for pre-processing images [17, 18, 19, 20, 21].

Although image processing includes different steps, segmentation is the most important one in medical imaging, aiming at separating images into regions that are meaningful for a specific task, such as the detection of organs or the computation of some metrics.

Segmentation approaches can be classified into several categories on the basis of the involved features and the typology of implemented technique. It has to be noticed that features of interest include pixel intensities, gradient magnitudes, or measures of texture. Segmentation techniques applied to these features can be broadly classified into three categories: region-based,

7

edge-based, or classification ones [20]. On the basis of this classification, region-based and edge-based segmentation techniques explore intra-region similarities and inter-region differences between features, whereas a classification technique assigns class labels to individual pixels or voxels based on feature values.

In some case, grey-level thresholding is a simple but effective segmentation method [22]. Thresholding may be performed at global or local level, i.e., thresholds can be selected equal to a constant value throughout the image, or spatially varying by computing different thresholds for each subsection of the image. Thresholding methods can also be categorized as point-based or region-based techniques. Region-based methods compute the value of a proper threshold not only on the basis of the grey-level of an individual pixel, but also considering the properties of its neighbourhood. Whether local or global, point-based or region-based, thresholds are typically estimated from the intensity histogram using different approaches.

Moreover, an a priori knowledge could be necessary to perform an appropriate segmentation, due to the fact that noise, artifacts or other issues could make segmentation a tricky task, not simply achievable using only information coming from grey level values. In [23] these problems are overcome by considering deformable and active models or atlas-based methods.

Classification algorithms are frequently used for segmentation too. Supervised classification for segmentation requires training data from users to enable classifiers to learn how to label each pixel of the input images. On the other side, unsupervised classifiers are based on cluster analysis to discriminate natural structures in the input images starting from the data themselves. In recent years, however, segmentation methods based on Deep Learning architectures have been introduced [24]. Since classification architectures are used to classify Regions Of Interest (ROIs) in CAD system, a detailed discussion about the topic is dealt with in Section 2.4.

The previous processing phases are preparatory for the extraction of ROIs containing the areas to be classified. In detail, the output from the segmentation task is generally a binary mask, which is superimposed on the starting image in order to filter-out all undesired areas [25]. The detected ROIs are subsequently considered on the basis of the classification methodologies used in the following step. More in detail, a further step for the extraction of features is necessary in case of traditional approaches for classifications, such as by means of Artificial Neural Networks (ANNs) of Support Vector Machines (SVM). On the contrary, in Deep Learning approaches, e.g., con-

sidering Convolutional Neural Networks, a subsequent step for the extraction of features is not necessary, since these networks process images as inputs. Medical imaging is essential in many fields of medical research and clinical practice, because it greatly facilitates early and accurate detection and diagnosis of diseases. In particular, contrast enhancement is essential for an optimal image quality and visibility.

Processing methods for enhancing morphological features of masses and other abnormalities in medical images are also very useful [26]. The morphological method involves two steps: (1) selective extraction of target features by mathematical morphology and (2) enhancement of the extracted features by two contrast modification techniques. The goal of the analysed method [26] consists in enabling the enhancement of fine morphological features of a lesion region with a high suppression of surrounding tissues. The effectiveness of the method is evaluated in quantitative terms of the contrast improvement ratio. Results clearly show that the method outperforms five conventional contrast enhancement methods. The effectiveness and usefulness of the proposed method have been further demonstrated by the application to three types of medical images: a mammographic image, a chest radiographic image, and a retinal one. As a conclusion it can be affirmed that the proposed method enables the specific extraction and enhancement of mass lesions, which is essential for a clinical diagnosis based on medical image analysis. Thus, the method can be expected to achieve an automatic recognition of lesion locations and a quantitative analysis of lesion morphology. Now, concerning with liver segmentation, algorithms can be categorized according to the amount of involved user inputs: manual, semi-automated and fully automated. Manual segmentation is considered the "gold standard" in clinical practice and research, but is expensive and time-consuming. The increase of automated segmentation approaches is more robust, but may suffer from certain segmentation pitfalls. Thus, emerging applications of segmentation include surgical planning and integration with MRI-based biomarkers.

2.3. Feature Extraction

In this section, the importance of identifying appropriate features from medical images capable of characterizing and discriminating classes of interest will discussed.

For example, breast cancer segmentation could be advantaged by combining morphological features with texture features. In [27] the authors have developed a fully automated, three-stage segmentation method that includes

clustering, active contour, and spicularities detection stages. After segmentation, morphological features describing the shape of the mass were extracted. Texture features were also extracted from a band of pixels surrounding the mass. Stepwise feature selection and linear discriminant analysis are employed in the morphological, texture, and combined feature spaces for classifier design. The improvement obtained by supplementing texture features with morphological features in classification was statistically significant. In this work the leave-one-case-out discriminant scores from different views of a mass is combined to obtain a summary score for classifying a mass as malignant or benign.

In [28] a Computer-Aided Diagnosis (CAD) system based on shape analysis is proposed, which proves to be highly accurate in evaluating breast tumours. However, it takes considerable time to train the classifier and diagnose breast tumours, because the extraction of morphologic features require a lot of computation. Hence, to develop a highly accurate and quick CAD system, texture and morphologic features of ultrasound breast tumour imaging are combined to evaluate breast tumours and reveal that the proposed system reduces the training time compared to systems based only on the morphologic analysis.

According to literature, there are several sets of features that could be used to characterize regions of interest. From a general point of view, the features may be distinguished between *global* and *local*, based on the localization of the information used to compute: global features are function of the whole image, whereas local features are a function of a local image region.

Among global features, the most used are Haralick features [29] (Table 1), Local Binary Patterns (LBP) [30] and Threshold adjacency statistics (TAS) [31]. On the contrary, the most used set of local features are the Speeded-Up Robust Features (SURF) [32].

Moreover, there are some other descriptors useful for the characterization of neoplasias or lesions based on descriptors of shape that could be computed from Regions of Interest. In Fig.5 some examples of tumour classification starting from the shape in benign and malignant cases is represented.

2.4. Classification

In the last years, a relevant number of studies have been proposed, from a classification point of view. In most cases, the design of CAD systems is based on a supervised learning approach, using Artificial Neural Networks (ANNs) or Support Vector Machines (SVMs), as well as Swarm Intelligence

Table 1: 14 statistics that can be calculated from the co-occurrence matrix with the intent of describing the texture of the image from [29].

|	
Angular Second Moment	$\sum_i \sum_j p(i,j)^2$
Contrast	$\sum_{n=0}^{N_g-1} n^2 \{\sum_{i=1}^{N_g} \sum_{j=1}^{N_g} p(i,j)\}, |i-j| = n$
Correlation	$\frac{\sum_i \sum_j (ij)p(i,j) - \mu_x \mu_y}{\sigma_x \sigma_y}$ where μ_x, μ_y, σ_x and σ_y are the means and std. deviations of p_x and p_y the partial probability density functions
Sum of Squares: Variance	$\sum_i \sum_j (i-\mu)^2 p(i,j)$
Inverse Difference Moment	$\sum_i \sum_j \frac{1}{1+(i-j)p(i,j)}$
Sum Average	$\sum_{i=2}^{2N_g} i p_{x+y}(i)$ where x and y are the coordinates (row and column) of an entry in the co-occurence matrix, and $p_{x+y}(i)$ is the probability of co-occurence matrix coordinates summing to $x+y$
Sum Variance	$\sum_{i=2}^{2N_g} (i-f_8)^2 p_{x+y}(i)$
Sum Entropy	$-\sum_{i=2}^{2N_g} p_{x+y}(i) log\{p_{x+y}(i)\} = f_8$
Entropy	$-\sum_i \sum_j p(i,j) log(p(i,j))$
Difference Variance	$\sum_{i=0}^{N_g-1} i^2 p_{x-y}(i)$
Difference Entropy	$-\sum_{i=0}^{N_g-1} p_{x-y}(i) log\{p_{x-y}(i)\}$
Info. Measure of Correlation 1	$\frac{HXY - HXY1}{max\{HX, HY\}}$
Info. Measure of Correlation 2	$(1 - \exp{-2(HXY2 - HXY)})^{\frac{1}{2}}$ where $HXY = -\sum_i \sum_j p(i,j) log(p(i,j))$, HX, HY are the entropies of p_x and p_y, $HXY1 = -\sum_i \sum_j p(i,j) log\{p_x(i)p_y(j)\}$, $HXY2 = \sum_i \sum_j p_x(i)p_y(j) log\{p_x(i)p_y(j)\}$
Max. Correlation Coeff.	Square root of the second largest eigenvalue of Q where $Q(i,j) = \sum_k \frac{p(i,k)p(j,k)}{p_x(i)p_y(k)}$
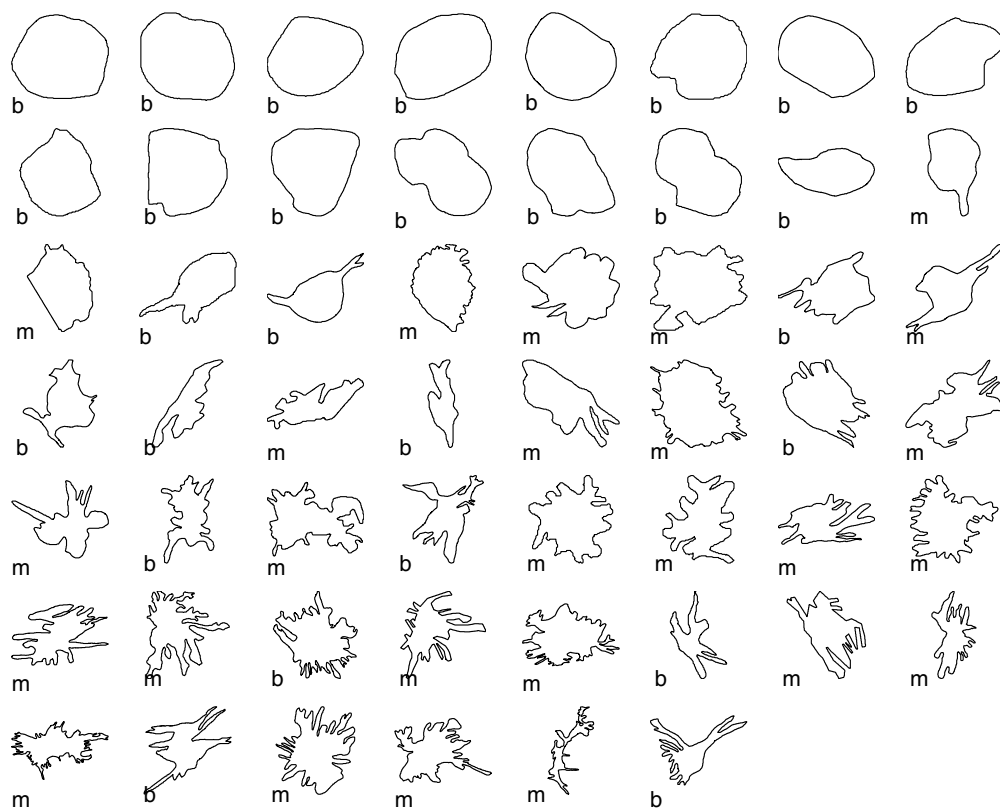
Figure 5: Tumour diagnosis from contours of breast masses: (b) benign masses, (m) malignant tumours. Image from [33].

or simpler Linear Discriminant Analysis (LDA) [34, 35, 36, 37, 38, 39, 40, 41, 42, 43, 44, 45, 46, 47, 48, 49, 50] classifiers built on radiologists' gold standard labelling.

In particular, ANNs may be classified in several ways based on:

- the function that the ANN is designed to serve (e.g. pattern association, clustering);

- the degree (partial/full) of connectivity of the neurons in the network;

- the direction of flow of information within the network (recurrent and non-recurrent);

- the type of learning algorithm, which represents a set of systematic equations that use the outputs obtained from the network along with an arbitrary performance measure to update the internal structure of the ANN;

- the learning rule, as known as the diving engine of the learning algorithm;

- the degree of learning supervision needed for ANN training.

In general, supervised learning involves the training of an ANN with the correct answer (i.e, target outputs) being given for every example, and using the deviation error of the ANN solution from corresponding target values to determine the required amount by which each weight should be adjusted. On the other side, the unsupervised learning does not required a correct answer for the training examples. However the network arranges examples into clusters based on their similarity or dissimilarity [51], through exploring the underlying structure in data and the correlation between the various examples themselves.

The development of an ANN requires partitioning of the parent database into:

- **training set**: should include all the data belonging to the problem domain and is used in the training phase to update the weights of the network;

13

- **validation set**: is used after selecting the best network to further examine the network or confirm its accuracy before being implemented in the neural system and/or delivered to the end user;

- **test set**: is used during the learning process to check the network response for untrained data.

The data used in each set (training, validation and test) should be different from each other. There are no mathematical rules but only some rules of thumb derived from experience and analogy between ANNs and statistical regression for the determination of the required sizes of the training, validation and test set. In particular, cross-validation (CV) is a popular strategy for algorithm selection. The main idea is to split parent dataset, once or several times, for estimating the risk of each algorithm. The popularity of CV mostly comes from the "universality" of the data splitting heuristics. Nevertheless, some CV procedures have been proved to fail for some model selection problems, depending on the goal of model selection, estimation or identification. Furthermore, many theoretical questions about CV remain widely open, as reported in [52, 53, 54, 55, 56, 57, 58].

The advent of new competitive imaging modalities for the same diagnostic problem has led to performance of many studies involving comparisons of the information obtained from these imaging techniques. Several of these comparisons have used Receiver Operating Characteristic (ROC) curves [59, 60, 61]. In other words, the main goal of these studies is to judge the discrimination ability of various statistical methods that combine various clues and test results for predictive purposes. In [62], the authors undertake the investigation about the issues related to the use of the statistical techniques proposed for comparing the information obtained from imaging technique with ROC curves. The intuitive result that the authors show is that in the rating method reported in [63], conventionally employed for analysing imaging modalities using the ROC curve approach, the area under the ROC curve represents the probability that a random pair of normal and abnormal images will be correctly ranked as to their disease state. In particular, the authors emphasized that this probability only conveys the intrinsic potential for discrimination with sensitivity and specificity weighted equally; other external decision factors that influence diagnostic performance include the real mixture of diseased and non-diseased patients and the relative costs of the two types of diagnostic errors.
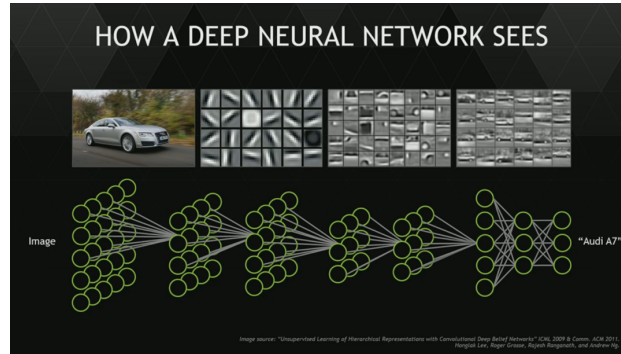
Figure 6: A representation of the CNN layers. Image from [68]

In literature, two different classes of ANNs could be identified on the basis of the number of hidden layers: Shallow and Deep Neural Networks. In details, ANNs with a single hidden layer are named Shallow Neural Networks, whereas a Deep architecture has a number of hidden layers greater than one (Fig. 7).

Regarding deep architectures, different strategies have been introduced in the literature so far; the success of deep networks in image processing is mainly due to the spread of Convolutional Neural Networks (CNNs). These kind of architectures are able to make a decision (i.e. classify) working directly on a raw image given as input to the network [64, 65, 66]. In fact, a CNN is capable of automatically extracting some descriptors (feature learning capability) of an image, thus eliminating the development of algorithms for the processing of images for the extraction of the so-called "hand-crafted" features [67] necessary to a classical classifier, such as ANN or SVM. The general architecture of a Convolutional Neural Network is shown in Fig. 6; it is a combination (which depends on the specific implementation) of convolutional layers, relu layers and pooling layers followed by a fully connected layer (as in classic multi-class ANNs).

Recent works reported the differences, in terms of performance, between shallow and deeper neural networks architectures 7, by highlighting the strengths and weaknesses of both strategies for classification [69, 70, 71]. According to literature, a sufficiently wide shallow neural network could approximate any (reasonable) function given enough neurons, so there is not an objective motivation to prefer Deep Neural Networks at all. In addition, the quality of the final generalisation properties of ANNs strictly depends on
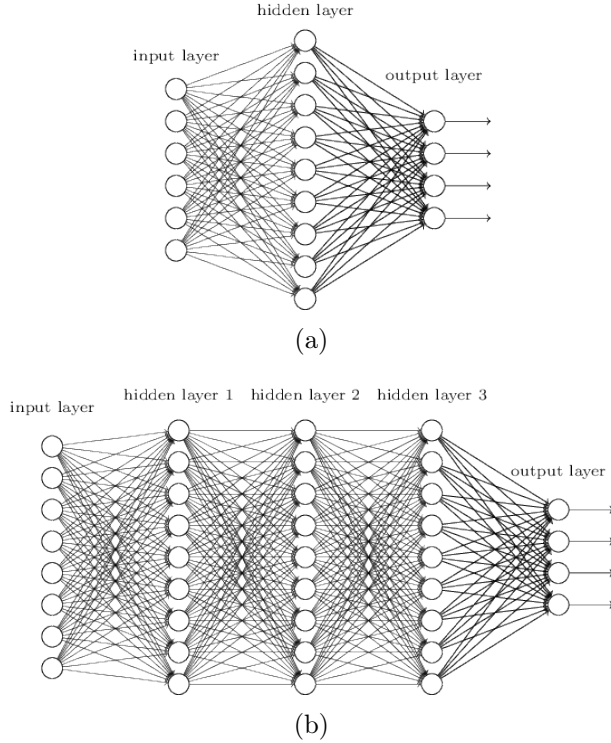
15

Figure 7: Architectural differences between (a) shallow and (b) deep neural networks. (Adapted from Nielsen [73] under Creative Commons Attribution-Non Commercial 3.0 Unported License)

.

the significance and classes-balance of the available training data [72].

However, a huge number of neurons for a single layer architecture increases the number of parameters to be tuned during the training phase, with the risk of over-fitting the data [74]. Making ANNs deeper, by adding multiple layers, allow the classifier to learn features at different levels of abstraction, on the bases of the number of hidden layers, leading to stronger capabilities of generalisation.

In recent years, Deep Learning (DL) and Convolutional Neural Networks (CNNs) have been used in many applications for images segmentation and classification, including the medical field with more than 100 papers in just four years as reported in Fig. 8, in particular for breast cancer [75, 76, 77, 78, 79, 80, 81, 82, 83, 84, 85, 86, 87, 88, 89, 90, 91, 92, 93].

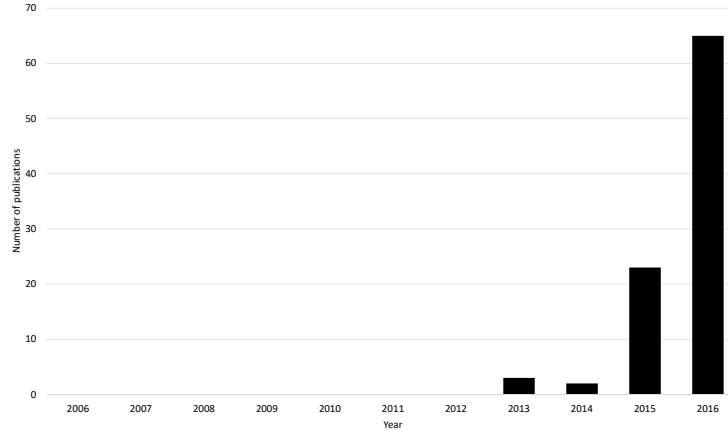Convolutional Neural Networks are powerful architectures that may be

Figure 8: Number of publications per year from 2006 to 2016. Topic: Convolutional Neural Network & Medical Imaging. Indexes: SCI-EXPANDED, SSCI, A&HCI, CPCI-S, CPCI-SSH, ESCI.

used in three different ways:

- **Training from scratch**: as for ANNs, Convolutional Neural Networks may be created from scratch, designing the overall architecture and providing enough samples as input for training. Generally, this process takes a lot of time using large datasets with several classes.

- **Transfer Learning or Fine-Tuning**: this approach allows to use an available pre-trained model for classification purposes different from the original classes. In details, it is possible to fine-tune the classification layer of a CNN to predict new classes given as input.

- **Features Extractors**: in addition to the previous ways, it is possible to remove the classification layer from the CNN and consider the output as features describing the input image computed automatically from the network. This process is iterative, so it is possible to remove more (intermediate) layers based on the desired level of abstraction of the features.

17

Regardless of the adopted strategy for classification, a diffused structure for representing the classifiers capability to discriminate among the different classes is the confusion matrix. Limiting the analysis to a binary classifier with Positive and Negative classes, a representation of a confusion matrix is reported in Table 2, where:

- **TP**: is the number of instances correctly classified as Positives;

- **TN**: is the number of instances correctly classified as Negatives;

- **FP**: is the number of Negatives instances classified as Positives;

- **FN**: s the number of Positives instances classified as Negatives.

Table 2: A representation of a confusion matrix.

		True Condition	
		Positive	Negative
Predicted Condition	**Positive**	TP	FP
	Negative	FN	TN

Based on the representation in Table 2, several metrics may be computed for the performance evaluation of classifiers [94, 95, 96]. The most used in literature are Accuracy, Sensitivity (or True Positive Rate) and Specificity (or True Negative Rate) reported in Equation 1, 2 and 3.

$$Accuracy = \frac{TP + TN}{TP + TN + FP + FN} \tag{1}$$

$$Sensitivity = \frac{TP}{TP + FN} \tag{2}$$

$$Sensitivity = \frac{TN}{TN + FP} \tag{3}$$

3. Breast Cancer

The high incidence of breast cancer in women (more than 25% of cancers affecting women is breast cancer [2]) and the ever-increasing life expectancy of population require an accurate assessment of the breast glands with imaging techniques. In this field, mammography represents the gold standard imaging tool [97]; in fact, mammographic examinations are used in several screening programs thanks to the capability to perform a very early detection, whereas Magnetic Resonance (MR), Computer Tomography (CT) or Digital Breast Tomosynthesis (DBT) techniques are necessary to perform a more in-depth analysis of risky cases, or for the follow-up of treated patients [98]. In recent years, several works have been presented dealing with breast lesions detection and classification considering deep strategies for classification.

In [99] Samala *et al.* designed a DL-CNN architecture for breast micro-calcification classification. The authors compare a DL-CNN architecture, whose optimal architecture was obtained by varying among 216 combinations of parameters in the network (e.g., the number of filters and the filter kernels) and analysing the effects of their variation in the parameter space, and a previously designed Artificial Neural Network performing convolution on the input images. Results show a statistically significant improvement since the Areas Under the Curve (AUCs) of the first CNN and the subsequent DL-CNN are equal to 0.89 and 0.93, respectively.

Kallenberg *et al.* present a method capable of learning from features at multiple scales hierarchy not labelled data addressing two different tasks: (i) breast density segmentation and (ii) scoring of mammographic texture [100]. The authors report that the scores obtained by performing the proposed approach, based on automatic learning, have a high correlation with the ones obtained with the manual approach. Furthermore, the learned texture scores are predictive of breast cancer.

3.1. Experimental Studies

In the following sections, two different works for detecting and classifying breast lesions will be analysed and discussed. In particular, a supervised approach for the detection and classification of breast lesions from MR images will be introduced in Section 3.1.1, whereas a supervised approach based on deep architectures for the extraction of features in order to classify with simpler non-neural strategies will be discussed in Section 3.1.2.

3.1.1. Magnetic Resonance

In [34], a CAD system for detecting and classifying breast lesions in images acquired via Magnetic Resonance is presented. The workflow followed in [34] is reported in Fig. 9 and will be discussed in this section.
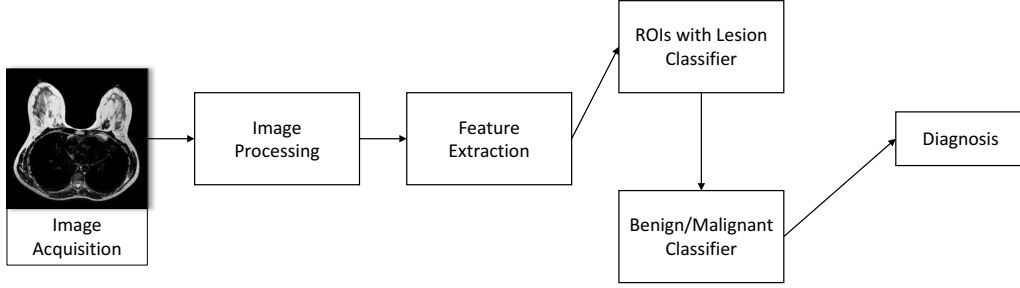

Figure 9: Workflow for breast lesion classification.

The acquisition phase was conducted following the standard procedure for breast cancer diagnosis, which consists of as follows:

- Transverse short TI inversion recovery (STIR) turbospin-echo (TSE) sequence (TR/TE/TI = 3.800/60/165 ms, field of view (FOV) = 250x450 mm (APxRL), matrix 168x300, 50 slices with 3-mm slice thickness and without gaps, 3 averages, turbo factor 23, resulting in a voxel size of 1.5 x 1.5 x 3.0 mm^3; acquisition time: 4 minutes);

- Transverse T2-weighted TSE (TR/TE = 6.300/130 ms, FOV = 250x450 mm (APxRL), matrix 336x600, 50 slices with 3-mm slice thickness and without gaps, 3 averages, turbo factor 59, SENSE factor 1.7, resulting in a voxel size of 0.75x0.75x3.0 mm^3; acquisition time: 3 minutes);

- Three-dimensional dynamic, contrast-enhanced (CE) T1-weighted high resolution isotropic volume (THRIVE) sequences (TR/TE= 4.4/2.0 ms, FOV = 250x450x150 mm (APxRLxFH), matrix 168x300, 100 slices with 4-mm slice thickness, spacing between slices: 2 mm; turbo factor 50, SENSE factor 1.6, 6 dynamic acquisitions, resulting in 1.5 mm^3 isotropic voxels, a dynamic data acquisition time of 1 min 30 s, and a total sequence duration of 9 min).

In details, the first step of the considered work consisted in the preprocessing of acquired images; after a simple rescaling of the grey level of pixels,

an algorithm for the masking of the thorax in all the slices is performed, thus filtering out all the structures external to the breasts. As reported in Fig. 10, three points are computed to generate a parabola with the vertex on the sternum (point A) and passing through the side edges of the chest (points B and C).
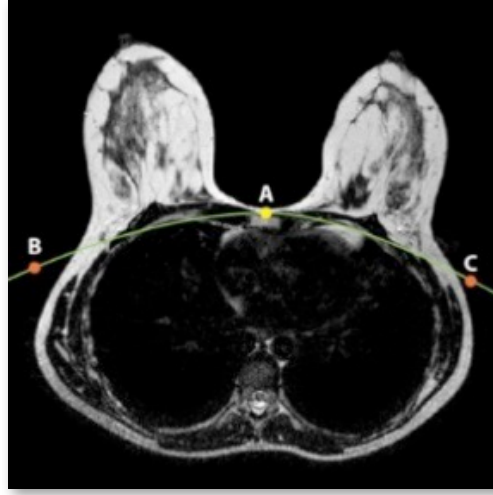

Figure 10: Algorithm output for thorax masking. The reference points for parabola generation are A, B and C.

A segmentation phase, necessary for the removal of all the uninteresting parts of the image, is subsequently performed. In particular, a thresholding operation is performed considering the 95th percentile of the grey levels histogram of the images acquired without contrast medium (CM). Then, areas with diameter below 5 mm are removed and the obtained mask is applied to the starting image in order to extract the regions of interest. The remaining areas were characterized considering 10 features which were:

- **F1**: size in mm^2 of the suspicious lesion;

- **F2, F3**: average value of the grey levels of images with and without CM in ROIs, to determine areas with gray intensity different from standard ones;

- **F4, F5**: standard deviation value of the gray levels of images with and without CM in ROIs, respectively;

- **F6**: circularity expressed as $4\pi(\frac{A}{p^2})$ where A = ROI_area and p = ROI_perimeter;

- **F7**: aspect ratio intended as $\frac{majorAxis}{minorAxis}$;

- **F8**: eccentricity of the ellipse whose second order moments coincide with those of each ROI;

- **F9**: solidity, defined as ratio of the area of the ROI and the area of convex hull;

- **F10**: convexity (or edge roughness), given by the ratio between the perimeter of the convex hull and the one of the ROI.

After the extraction of the features, two different Artificial Neural Networks can be designed using an evolutionary strategy, as reported in [35]. The first ANN is designed to discriminate among lesions and other structures (e.g. vessels), while the second one is used to classify benign and malignant lesions, taking the same set of features of the regions classified as lesions in the previous step as input.

In particular, regarding the first classifier, the generated dataset is balanced with a Synthetic Minority Over-sampling Technique (SMOTE) to increase the number of patterns characterizing lesions until the amount of negative cases to achieve better classifier performance [101]. In both cases, performances were measured in terms of Accuracy, Sensitivity and Specificity as reported in Section

The results obtained in both cases are reported in Table 3, and 4. In details, the reported tables show Accuracy, Sensitivity and Specificity as mean values obtained performing 100 iterations of training, validation and test of ANN, considering a different random permutation of the input dataset at each iteration.

The reported results show that a supervised machine learning approach for the detection of breast lesions from MR images and the subsequent classification between benign and malignant is consistent, and shows good performance, especially from a False Negative reduction perspective.

3.1.2. Digital Tomosynthesis

Digital Breast Tomosynthesis (DBT) has been recently introduced for breast cancer screening and detection, and consists in a promising inno-

Table 3: Results obtained in [34] for the discrimination between ROIs with and without lesions.

	Min	Max	Mean
Accuracy	*0.9624*	*0.9849*	*0.9736 ± 0.0044*
Sensitivity	*0.9592*	*0.9958*	*0.9791 ± 0.0075*
Specificity	*0.9459*	*0.9892*	*0.9684 ± 0.0075*

Table 4: Results obtained in [34] for the discrimination between benign and malignant lesions.

	Min	Max	Mean
Accuracy	*0.7308*	*1*	*0.8977 ± 0.0584*
Sensitivity	*0.6923*	*1*	*0.8908 ± 0.1021*
Specificity	*0.7692*	*1*	*0.9046 ± 0.0875*

vative radiological technique for early diagnosis and staging. DBT produces a limited angle cone beam tomosynthesis of the breast glands and has demonstrated to have a higher accuracy if compared to the most commonly used bi-dimensional imaging techniques, such as mammography, CT or MR [97, 102, 103, 104]. After the acquisition of multiple thin and high-resolution images, a 3D model of the breast is created, reducing the effect of tissue superimposition, too [105]. DBT improves the visualisation of masses and architectural distortions. In particular, the edges of the breast lesions are better defined, and this allows an improvement of the final diagnosis [106].

In [107], a CAD system to support the classification of three different kinds of lesions was designed.

As for the previous cited work, an image processing step performing segmentation was needed to extract candidate regions of interest containing suspicious lesions. In details, the extracted ROIs are labelled according to the classification by radiologists in 4 classes:

1. **None**: segmented ROI not containing any kind of lesion (Fig. 12(a));

2. **Ori**: segmented ROI containing an irregular opacity (Fig. 12(b));

3. **Oro**: segmented ROI containing a regular opacity (Fig. 12(c));

4. **Ost**: segmented ROI containing a stellar opacity (Fig. 12(d)).
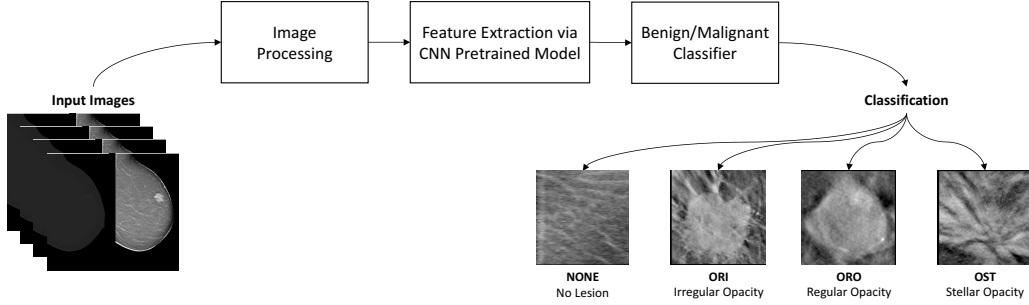
23

Figure 11: Workflow for breast lesion classification.

Differently from the work described in the previous section, in [107], the extraction of features describing the segmented ROIs is performed following two different approaches:

- Several pre-trained models of Convolutional Neural Networks were used as automatic features extractors by pruning the CNN architectures at certain levels of depth;

- Hand-crafted morphological and textural features were computed using the Grey Level Co-occurrence Matrix (GLCM) [29, 108, 109].

Since the strategies for features extraction are different, also the classification step was performed following different approaches.

In particular, two different Artificial Neural Networks are designed by an evolutionary approach to discriminate among the four classes taking the hand-crafted features as input. In a first step, Ori, Oro and Ost classes have been grouped into a single one (P), while None is the second class (N); in this case, a binary classifier is used and the obtained performance are reported in Table 5. Subsequently, the second ANN is used to discriminate among the four classes, but the obtained Accuracy was lower than the binary classifier (74.84 % ± 4.89).

This behaviour reveals predictable and reasonable considering the way in which ANNs were designed and optimized: the extraction process of the most discriminant features heavily influences the overall capabilities of the classifier. In this case, the features used as inputs showed good results to discriminate binary class samples, while these did not provide enough information to correctly describe all the different kinds of lesions in the multi-class approach.
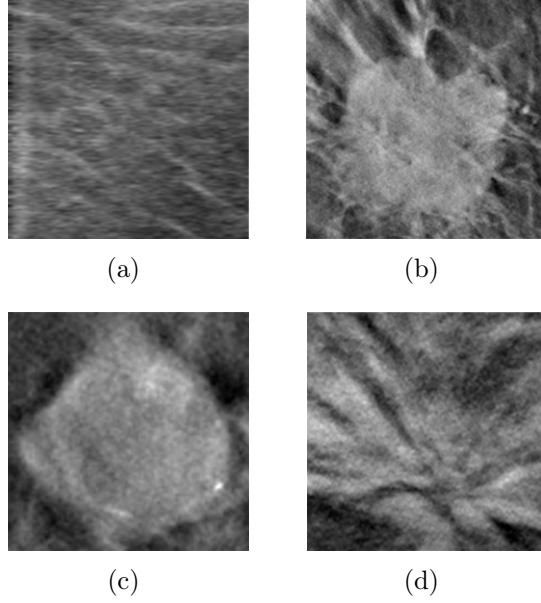
Figure 12: Images extracted after the segmentation phase: (a) ROI with no lesions; (b) ROI with irregular opacity; (c) ROI with regular opacity; (d) ROI with stellar opacity.

Table 5: Results obtained for binary classification.

	Accuracy	Sensitivity	Specificity
Mean	*84.19 %*	*85.90 %*	*82.82 %*
Standard Deviation	*3.06*	*5.33*	*5.17*

Regarding CNNs as feature extractors, several pre-trained models are considered, which were: GoogLeNet, ResNet, AlexNet, VGG-verydeep, VGG-F, M and S [65, 110, 111, 112, 113, 114, 115, 116].

In the second approach, the dataset is constituted by the set of features extracted by the CNN models. The output of the CNN models (in other words, their final activations) is used to train several non-neural learners, which were: Linear Support Vector Machine (Linear SVM), K-Nearest Neighbor (KNN), Naïve Bayes, Decision Tree and Linear Discriminant Analysis (LDA) [117, 118, 119, 120, 121, 122].

Final tests were performed on all the considered CNN architectures. In order to improve the overall performance, several tests for dataset processing are performed; in particular, Activation Normalization and Images Augmentation are explored leading to a slight improvement in all the architectures. Finally, since VGG-F, VGG-S and VGG-S show the higher mean accuracies and the lowest processing time, they are considered for final evaluation.

The results reported in [107] (Table 6) show that Naïve Bayes classifier is not recommended in this classification; Decision Trees allow to improve the mean accuracy in comparison to NaÃŕve Bayes, but it is far to be considered as a reliable classifier. The linear classifiers (SVM and LDA) further increased the performance, but better results were obtained from KNN classifiers. In this case, mean performances reached very good levels of accuracy, specificity and sensitivity with low variability. Furthermore, to substantiate the high level of performance in terms of accuracy, it is worth to mention that sensitivity and specificity for positive samples reveal higher than 95 %, as reported in Table 7 where results are calculated using a 1-vs-all approach.

Table 6: Results of the selected pre-trained CNNs used as features extractor, training several learners with normalization and augmented images.

	KNN	LDA	LINEAR SVM	NAÏVE BAYES	DECISION TREES
VGG-F	91.63 ± 0.41	64.57 ± 0.66	67.29 ± 2.02	43.82 ± 0.59	59.68 ± 1.07
VGG-M	90.74 ± 0.48	66.25 ± 0.60	69.50 ± 2.16	42.85 ± 0.57	57.03 ± 0.98
VGG-S	92.02 ± 0.48	65.24 ± 0.80	68.84 ± 1.89	44.89 ± 0.60	56.16 ± 0.93

Table 7: Sensitivity and Specificity for the lesions evaluated through 1-vs-all approach.

	Ori vs all		Oro vs all		Ost vs all	
	Sensitivity	*Specificity*	*Sensitivity*	*Specificity*	*Sensitivity*	*Specificity*
VGG-F	*98.67 %*	*97.07 %*	*96.01 %*	*95.98 %*	*97.24 %*	*96.93 %*
VGG-M	*98.14 %*	*96.64 %*	*95.00 %*	*95.76 %*	*97.18 %*	*96.62 %*
VGG-S	*98.36 %*	*97.13 %*	*95.61 %*	*96.33 %*	*96.67 %*	*97.25 %*

4. Liver Carcinoma

As for breast cancer, liver cancer shows an extremely high mortality worldwide [2]. In recent years, several works have been presented dealing with detection and classification of hepatic tumours considering different strategies for classification.

A method to segment liver and lesions automatically in CT and MRI abdomen images is proposed in [123] by using Cascaded Fully Convolutional Neural Networks (CFCNNs), which enable the segmentation of large-scale medical trials and quantitative image analyses. In particular, the authors focused on CT images and applied a CFCNN on CT slices, which can sequentially segment liver and lesions, leading to a significantly higher segmentation quality and showing interesting performance on a public challenge dataset.

Moreover, a Deep Convolutional Neural Network (DCNN) is developed to segment the liver in CT slices via an automatic procedure also in [124]. The same model has been subsequently employed for the classification of lesions, by considering images from the previous classification as inputs. The developed models have been evaluated using the Liver Tumour Segmentation Challenge dataset (LiTS) for the liver segmentation tasks. In this paper a DICE coefficient equal to 0.67 is reached, but the lesion classification performance is still low, as reported by the author himself.

Different machine learning techniques for diagnosis of liver disease and hepatitis disease are developed in [125]. It is observed that Functional Trees (FTs) provide 97.10 % of correctness for the liver disease diagnosis. The implemented feedforward neural network correctly classifies hepatitis disease as it provides 98 % accuracy. This survey highlights both advantages and disadvantages of considered algorithms [126, 127, 128, 129, 130, 131].

A new method for the automatic detection and segmentation of unknown cancers in longitudinal liver CT studies and for a burden quantification of tumours is presented in [132]. The considered inputs are the baseline/follow-up CT scans, the baseline delineation of tumours, and a tumour appearance

prior model. The outputs are given by new segmentations of tumours in the follow-up scan, tumour burden quantification in both scans, and the tumour burden change. The method intends to find new neoplasias by integrating information from the scans, the baseline tumours delineation, and a tumour appearance prior model in the form of a global CNN classifier. Reported results show that this method is superior to existing stand-alone/follow-up methods, with both high true positive rate and precision of 86 % on a dataset with 37 longitudinal liver CT studies with 246 tumours, among which 97 new ones.

A fully automatic framework for liver segmentation together with its tumour on contrast enhanced abdominal CT scans is developed in [133], which is based on three steps: i) a liver localization by a simple CDNN model; ii) a liver fine segmentation via a deeper CDNN model with doubled feature channels in each layer; iii) a tumour segmentation by a CDNN model with enhanced liver region as additional input feature. Considered CDNN models are fully trained in an end-to-end mode with minimum pre- and post-processing efforts. Furthermore, two CNNs are used for liver segmentation and metastases detection on CT examinations in [134]. Authors use CNN architectures based on a VGG 16-layer net as in [113]. In particular, the final classification layer is removed and substituted with a $(1\tilde{A}\mathring{U}1)$ convolution with channel dimension equal to 2 to predict scores for lesion or liver at each of the coarse output locations, followed by a deconvolution layer to up sample the coarse outputs to pixel-dense outputs, whereas all the intermediate fully connected layers are substituted with convolutional layers. Starting from the previous architectures, two variants are obtained linking lower layers to the final layer, which are FCN-8s DAG and FCN-4s DAG, respectively, and 3D information is also taken into account by considering adjacent slices as input to the network. Moreover, regarding with the segmentation phase, Dice index, Sensitivity and Positive Predictive Values (PPV) are used to evaluate the segmentation performance. In particular, higher values for all the three indexes are reached using the FCN-8s DAG combining information from the 2 adjacent CT slices of the considered one. Regarding the detection of metastases, instead, the True Positive Rate (TPR) and False Positive per Case (FPC) metrics are used for performance evaluation. In this case, the 3D information allowed to reach the highest performance with the FCN-4s architecture. Although the results obtained in this work are very promising, the dataset herein considered is small and needs to be increased to evaluate the robustness of the proposed algorithms.

A novel application of Convolutional Neural Networks (CNNs) is presented in [135] to segment liver tumours. In this work, this method is tested on 30 CT images using leave-one-out cross validation. The reported experiments show that the CNNs model produce an accurate and robust liver tumour segmentation. If compared to traditional machine learning methods, such as AdaBoost, RF, and SVM, the CNNs method seems to perform better. Limitations of CNNs are still found on segmenting tumours with inhomogeneous density and unclear boundary, especially the under-segmentation in the tumour adjacent to structures with similar densities.

In [136], several recent Computer Aided Diagnosis (CAD) systems used in the diagnosis of liver diseases have been discussed. This article reviews the various CAD systems used for the classification of liver diseases using CT scan images. The description of the tumour segmentation process focuses on the algorithm used to classify tumour and the corresponding results for all the considered works. However, this article does not consider the most modern deep learning classification techniques [137, 136, 138, 139, 140, 141, 142, 143, 144, 145, 146, 147].

The design and implementation of a CAD system consisting of liver and tumour segmentation, feature extraction and classification module is presented in [148], characterizing the CT liver tumour as haemangioma and hepatoma. The experiment results show that the classification accuracy of Fast Discrete Curvelet Transform (FDCT)-based feature extraction and classification is higher than the wavelet based method. Performance measurements can be increased by increasing the number of used samples. In this work, a pattern recognition network is used, which is a feed-forward network with tan-sigmoid transfer functions in both the hidden layer and the output one. The network has two output neurons, as there are two classes associated with each input vector. The performance of the classifier is evaluated by calculating accuracy (93.3 %), selectivity (90 %) and specificity (96 %) from the obtained confusion matrix. A Computer Aided Diagnosis (CAD) system based on texture features and a multiple classification scheme for the characterization of four types of hepatic tissue from Computed Tomography (CT) images has been presented in [149]. The proposed system has achieved a total classification performance of the order of 97 %. Regions of Interest (ROIs) corresponding to normal liver, cyst, haemangioma, and hepatocellular carcinoma, are drawn by an experienced radiologist on abdominal non-enhanced CT images. For each ROI, five distinct sets of texture features are extracted using the following methods: first order statistics, spatial grey

level dependence matrix, grey level difference method, Laws texture energy measures, and fractal dimension measurements. If the dimensionality of a feature set is greater than a predefined threshold, feature selection based on a Genetic Algorithm (GA) is applied. Classification of the ROI is then carried out by a system of five neural networks (NNs), each using as input one of the above feature sets. The members of the NN system (primary classifiers) are 4-class NNs trained by the backpropagation algorithm with adaptive learning rate and momentum. The final decision of the CAD system is based on the application of a voting scheme across the outputs of the individual NNs. The multiple classification scheme using the five sets of texture features results in significantly enhanced performance, as compared to the classification performance of the individual primary classifiers.

A pilot study for hepatocellular carcinoma grading and the evaluation of microscopic vascular invasion is proposed in [150] where a shallow artificial neural network is compared to linear models. The results obtained from ANN in terms of AUC and Accuracy are higher than the ones obtained from a linear logistic model in both HCC grading and MVI presence evaluation. In [151], biorthogonal wavelet based texture features are extracted and used to train the Probabilistic Neural Network (PNN) to classify the liver tumour as hepatocellular carcinoma, cholangio carcinoma, hepatocellular adenoma and haemangioma with better performance to help radiologists and medical specialists during their medical decision process. In particular, the PNN provides a general solution to pattern classification problem by following the probabilistic approach based on the Bayes formula. The performance of the PNN is compared with the performance of the Learning Vector Quantization (LVQ) Neural Network to prove the choice of the classifier. Moreover, the performance of the system are compared with the performance of the PNN in the grey level domain for the selected feature set to prove the choice of wavelet domain. In [152], 164 liver lesions (80 malignant tumours and 84 haemangiomas) are evaluated. The suspicious tumour region in the digitized CT image was manually selected and extracted as a circular sub image. The proposed pre-processing adjustments for sub images were used to equalize the information needed for a differential diagnosis. The auto-covariance texture features of sub image were extracted, and a support vector machine classifier identified the tumour as benign or malignant. The accuracy of the proposed diagnosis system for classifying malignancies is 81.7 %, the sensitivity is 75 %, the specificity is 88.1 %, the positive predictive value is 85.7 % and the negative predictive value is 78.7 %.

4.1. Experimental Studies

In the following sections, two specific works for detecting and classifying hepatocellular carcinoma will be analysed and discussed. In particular, a supervised approach based on the extraction of hand-crafted features for the detection and classification of HCCs from triphasic CT protocol will be introduced in Section 4.1.1, whereas a second approach based on a supervised Convolutional Neural Network will be discussed in Section 4.1.2.

4.1.1. Hand-crafted Features

In [153], the acquisition system is based on Computer Tomography, a medical imaging technique that is widely used for Hepatocellular Carcinoma (HCC) detection. In fact, CT, as well as MRI, are always required to determine the disease extension. In fact, both the techniques are considered as the gold standard for non-invasive evaluation of focal and diffuse diseases of liver and biliary tract [154, 155].

These CT scans are acquired with a 320 slices Scanner (Toshiba Aquilion One) after an automated injection of 1.5 ml/kg of iodinated contrast medium (Iomeprole 400 mgI/ml) through a 16G Needle in antecubital vein at a flow rate of 4ml/sec with the following protocol:

1. arterial dominant phase acquired 20 seconds after the aortic peak calculated by a bolus tracking system with a ROI positioned in the abdominal aorta at a trigger density of 150 Hounsfield Units (HU) (Fig. 13(a));

2. portal phase acquired 70 seconds after contrast injection;

3. equilibrium phase acquired 180 seconds after contrast injection Fig. 13(b)).

A double-step segmentation is carried out, after an image pre-processing phase performed through contrast enhancement, in order to improve the contrast of the CT images, and a cropping phase to reduce the amount of data to be processed. In particular, liver and HCC segmentation are performed.

Concerning with liver segmentation, the histogram of the slice with the largest connected portion of the liver is analysed to obtain the typical liver grey intensity. By means of this evaluation, local thresholding and morphological operations were performed, allowing to remove all the structures external to the liver. The segmentation result of the first CT slice is dilated and used as a binary mask for the previous and the following slices. Those
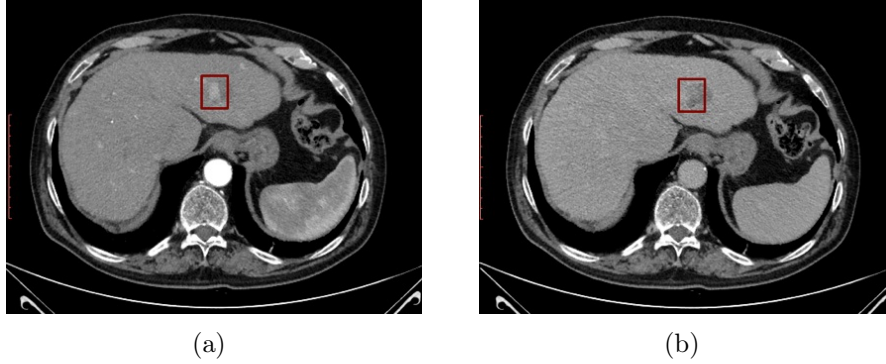
31

Figure 13: CT images acquired in the different phases: (a) Arterial phase; (b) Equilibrium phase. The square indicates the lesion in both phases.

slices were further segmented, and the method was iteratively propagated in both directions until the final slices are reached.

A similar procedure is performed for the HCC segmentation. Hepatocellular carcinoma are subsequently segmented using an innovative two-dimensional region growing algorithm which take into account images from both arterial and equilibrium phases. Some morphological operation are performed to refine the obtained Regions of Interest.

Textural features are then extracted using grey level co-occurrence matrices, as proposed by Haralick et al. [29] and derived from his works [108, 109] to describe ROIs. Each HCC was texturally described taking information from the two corresponding slices in both arterial and delayed phases.

Three different subsets of features were generated from the dataset:

1. 44 features obtained considering ROIs extracted from the two considered phases (specifically, 22 features extracted from each phase);

2. 22 features coming from an algorithm of ranking based on the relative entropy, also known as Kullback-Leibler distance or divergence [156];

3. 5 features in Haralick et al. (Contrast, Correlation, Energy, Homogeneity and Entropy) which have been used in similar previous work for blood vessels and tubules classification [25] and have shown good discrimination capabilities.

In this work, HCC grades, which could be classified into four classes (from grade 1 to grade 4) [157], have been grouped into two classes: grade 1/2 were

addressed like Negative Class, while grade 3/4 were addressed like Positive Class.

A binary classifier is designed to discriminate the two groups mentioned above using a mono-objective genetic algorithm (GA) [35]. Results, which are expressed in terms of mean values (± standard deviation), considering 100 iterations, for accuracy, specificity, and sensitivity, are reported in Table 8.

The results obtained in this work show that HCC classes can be discriminated by using the proposed set of extracted features: the HCC wash-in and wash-out dynamic suggests that this type of lesion can be characterized by processing textural differences considering the most important phases in the HCC dynamic.

Table 8: Results obtained for HCC classifier

Dataset	Accuracy	Sensitivity	Specificity
44 Features	0.758 ± 0.062	0.755 ± 0.122	0.739 ± 0.141
22 Features	0.763 ± 0.063	0.824 ± 0.089	0.698 ± 0.156
10 Features	0.799 ± 0.073	0.795 ± 0.015	0.804 ± 0.126

4.1.2. Deep Learning Approach

As for the previous work [153], in [158] the acquisition protocol is a triphasic CT acquisition characterized by an hyper-enhancement in the arterial phase followed by portal venous or delayed phase washout appearance.

To better understand the grading process, the following block diagram of the approach proposed in [158]is herein reported.

Regarding liver and HCC segmentations, the same procedures reported in the previous section were applied in [158], thus obtaining binary mask that were applied to CT images acquired during the arterial phase. A Convolutional Neural Network, specifically the Google Inception v3 implementation reported in [159], has been used by performing a retrain of the model using the created dataset of images as input.

The implemented CNN has been trained, validated and tested 100 times considering different permutations of the input dataset. The results reported in Table9 show that the implemented approach show high generalization performance regardless the input permutation; in fact, Accuracy, Sensitivity and Specificity are higher than 90 % maintaining low the standard deviation.
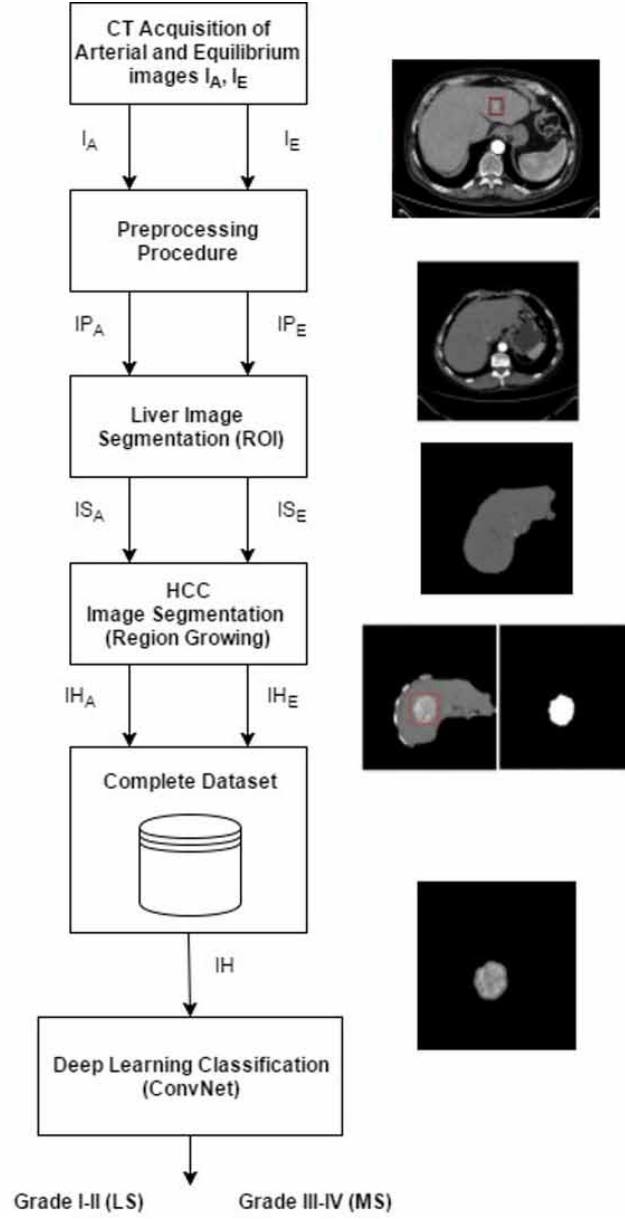
33

Figure 14: Block diagram of the proposed approach for hepatocellular carcinoma grading with samples of output images at each step.

34

Table 9: Results obtained for CNN classification.

	Accuracy	Sensitivity	Specificity
Mean	0.928	0.935	0.921
Standard Deviation	0.055	0.075	0.089

5. Blood Neoplasia

As reported in Section 1, the design of CAD systems for supporting clinical diagnosis of blood neoplasias is of fundamental importance since, in the most of cases, the invasiveness of diagnosis procedure is considerably reduced [160, 161, 162, 163, 164, 165, 166].

In [167] the proposed Super-Resolution Convolutional Neural Network (SRCNN) is considered, which surpasses the double-cubic baseline with just a few training iterations, and outperforms the Sparse Coding-based method (SC) with a moderate training. Performance may be further improved with more training iterations. In this work, different network structures are investigated, as well as parameter settings to achieve tradeoffs between performance and speed. Moreover, the proposed network is extended to cope with three-color channels simultaneously, and show better overall reconstruction quality.

Then, a deep learning method for single image super-resolution (SR) is proposed in [168]. The suggested method directly learns an end-to-end mapping between the low/high-resolution images and the mapping is represented as a deep Convolutional Neural Network (CNN) that takes the low-resolution image as the input and outputs the high-resolution one. Moreover, in the same paper traditional Sparse Coding-based SR methods are viewed as a deep convolutional network that jointly optimizes all layers, differently from traditional methods that handle each component separately. This deep CNN achieves fast speed for practical on-line usage, besides having a lightweight structure and presenting state-of-the-art restoration quality. In [168] different network structures are also investigated, together with parameter settings to achieve trade-offs between performance and speed.

A SVM classifier to perform White Blood Cell (WBC) classification is presented in [169]. The authors are particularly interested in the classification and counting of the five main types of white blood cells (leukocytes) in a clinical setting where the quality of microscopic imagery may be poor. The proposed approach is mainly composed of three steps: 1. Image ac-

quisition and discrimination of WBCs from RBCs (Red Blood Cells); 2. Feature extraction by Dual-Tree Complex Wavelet Transform (DT-CWT); 3. Classification by means of a Support Vector Machine (SVM) in the five WBC types. Experimental results indicate that current analysis presents remarkable recognition accuracy even in presence of poor quality samples and multiple classes.

5.1. Experimental Studies

In the following sections, two different approaches for detecting and classifying white blood cells (leukocytes) from peripheral blood smears will by analysed and discussed. In particular, the first approach is based on the extraction of hand-crafted features for a subsequent neural classifier (Section 5.1.1), whereas the second approach considers Convolutional Neural Networks as features extractors and a comparison between SVM classification and CNN classification considering images as input is shown in Section 5.1.2.

5.1.1. Hand-crafted Features

Observation under the microscope of Peripheral Blood Smears (PBS) is fundamental in haematology as analysis of leukocyte formula and of the morphological characteristics of blood cells (red blood cells, white blood cells, and platelets) provides useful information in the clinic.

The morphological evaluation of the WBC can help specialists diagnosing haematological pathologies such as leukaemia and non-haematological ones such as infectious mononucleosis.
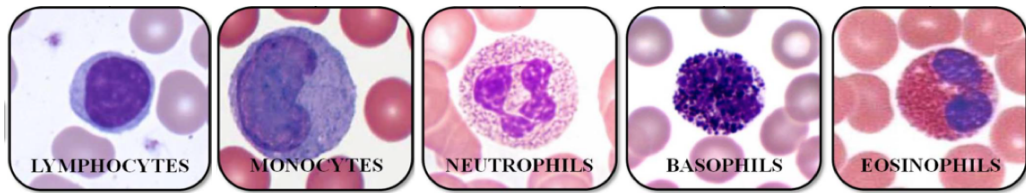

Figure 15: The five types of leucocytes to be classified: (from left to right) Lymphocytes, Monocytes, Neutrophils, Basophils and Eosinophils

In [170], image processing techniques with low computational requirements have been designed, together with a CAD system able to recognize all the five types of leukocytes (Fig. 15), named Neutrophils, Lymphocytes, Monocytes, Eosinophils and Basophils, improving the work by Hiremath *et*

36

al. [171], which considered a sub-sample of cells. The workflow followed in this approach is represented in Fig. 16.
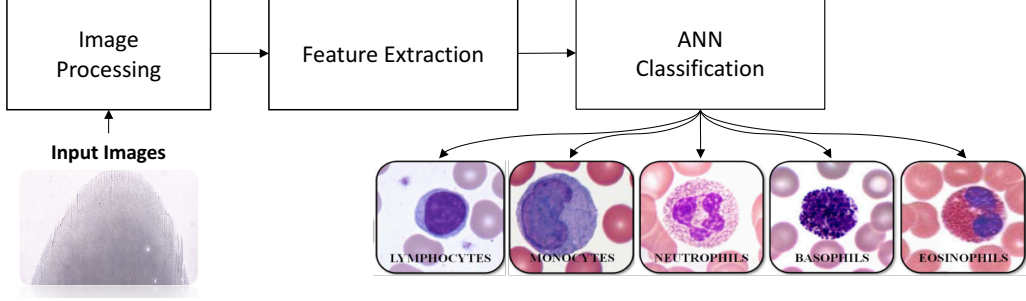

Figure 16: Workflow for leukocites classification considering hand-creafted features.

Blood Smears are digitally acquired using the microscope D-Sight 200 (www.menarinidiagnostics.it) featuring a 40x optical zoom, with a resolution of 0.25 μm/pixel and a *JPEG 2000* compression.

The leukocytes segmentation consists of three main steps able to detect the leukocytes position, the plasma and the leukocyte edge, respectively. In details, a colorspace conversion into Hue Saturation Value (HSV) space, a thresholding operation and morphological dilatation allow to generate a mask for the detection of nuclei positions in the image (Figure 17 and 18).
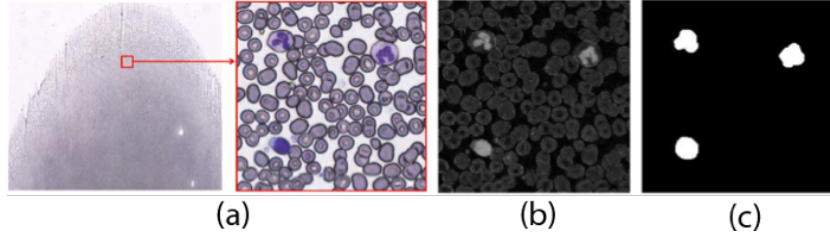
Figure 17: A representation of steps to obtain the nuclei mask; (a) Sub-image extraction. (b) S channel of HSV sub-image. (c) Nuclei mask obtained.

A thresholding operation considering the grey-scale histogram of each window containing a leukocyte allows subsequently to separate plasma (background) from the cell; finally, leukocytes edges are detected performing morphological operations on a mask obtained after a thresholding operation considering the blue channel of the RGB window.

37

Figure 18: Leucocyte's ROI and window extraction in one sub-image.

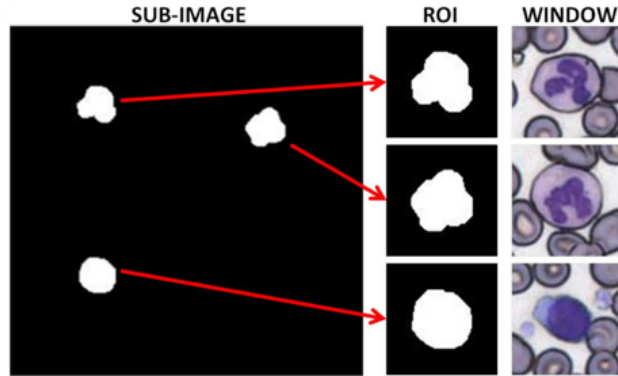In the described work, geometric, chromatic and texture-based features for blood cells representation have been extracted [172, 171, 173, 174] and an Artificial Neural Network and a Decision Tree have been designed to discriminate among the five different classes of leukocytes.

Results described in [170] are reported in Table 10 expressed in terms of Accuracy, Sensitivity and Precision on test set for the ANN classifier, only. In fact, the Accuracy reported in [170] for the Decision Tree is about 70 %, therefore much lower than the ANN.

Table 10: Accuracy, Sensitivity and Specificity for leukocytes classification evaluated through 1-vs-all approach.

	Accuracy	Sensitivity	Specificity
Neutrophils vs all	96.78 %	95.55 %	99.73 %
Lymphocytes vs all	96.78 %	98.81 %	96.06 %
Monocytes vs all	99.61 %	92.59 %	99.76 %
Eosinophils vs all	99.45 %	90 %	99.53 %
Basophils vs all	100 %	100 %	100 %

Reported results show that the proposed approach is suitable for white blood cells classification; it has to be noted that, even though the image processing procedure is very simple, performance reveal very high.

5.1.2. Deep Learning Approach

In a subsequent work [175], Convolutional Neural Networks have been proposed to perform leukocytes discrimination following two approaches.

In a first approach, a pre-trained Convolutional Neural Network have been deployed to extract features from the same set of segmented images of the previous work and then have been combined SVM to perform classification. The workflow followed in this approach is represented in Fig. 19.
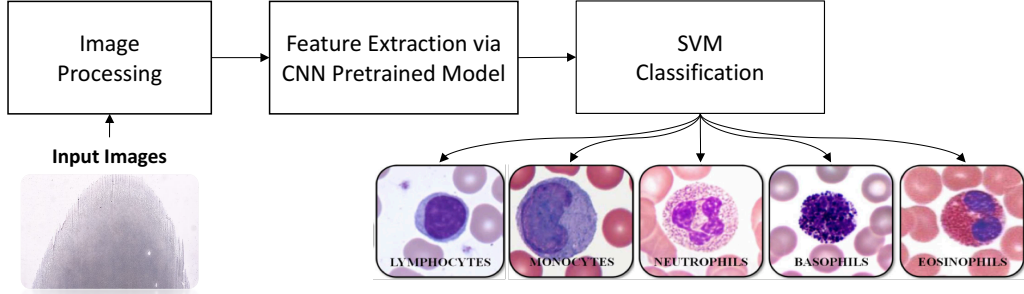

Figure 19: Workflow for leukocites classification considering CNN as feature extractors.

Then, the classification capabilities of the CNN have been explored to classify leukocytes using the segmented images as input. In this work, the considered model was the AlexNet by Krizhevsky *et al.* [65]. Differently from previous approaches, the workflow represented in Fig. 20 where the CNN is used for classification, shows that the features extraction step is skipped.
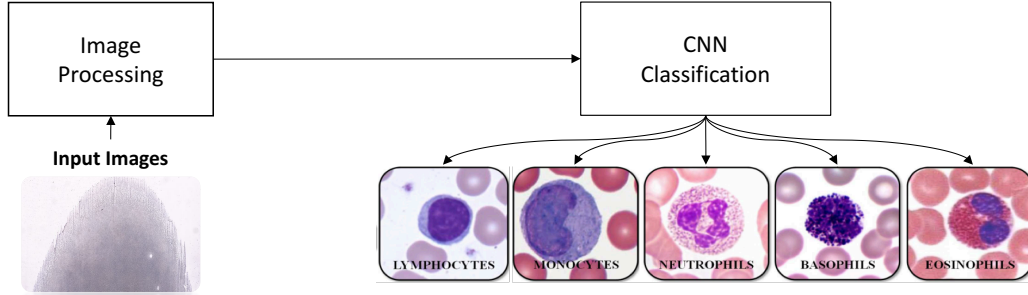
Figure 20: Workflow for leukocites classification using CNN for classification.

As for the previous work, the following Table 11 and 12 report the obtained results expressed in terms of Accuracy, Sensitivity and Precision on test set.

Reported results show that both the proposed approaches based on CNN seems very promising; in fact, the reported Accuracy values are always higher than 95 %. On the contrary, the Sensitivity and Specificity values for both

Table 11: Accuracy, Sensitivity and Specificity for leukocytes classification evaluated through 1-vs-all approach with SVM classifier.

	Accuracy	Sensitivity	Specificity
Neutrophils vs all	97.89 %	98.78 %	95.76 %
Lymphocytes vs all	98.59 %	97.93 %	98.83 %
Monocytes vs all	98.67 %	48.15 %	99.76 %
Eosinophils vs all	99.38 %	66.67 %	99.61 %
Basophils vs all	100 %	100 %	100 %

Table 12: Accuracy, Sensitivity and Specificity for leukocytes classification evaluated through 1-vs-all approach with CNN classifier.

	Accuracy	Sensitivity	Specificity
Neutrophils vs all	97.73 %	97.12 %	99.20 %
Lymphocytes vs all	97.73 %	99.70 %	97.03 %
Monocytes vs all	98.67 %	48.15 %	99.76 %
Eosinophils vs all	99.61 %	66.67 %	99.84 %
Basophils vs all	100 %	100 %	100 %

the approaches fluctuate depending of different kinds of cells. However, this result is explainable considering the number of samples for certain cells, such as Neutrophils and Lynphocytes, which is greater than the number of the other kinds of cells.

6. Conclusions and Discussion

Given the significant incidence both at global and at Italian level of the three neoplasias dealt with in this survey, it has to be noted that the scientific community has shown a great interest in identifying diagnostic and staging protocols which can enable a periodic monitoring of the course of the disease and, at the same time, be widely available for the population due to their reduced invasiveness. It has been shown that diagnosing through medical imaging currently reveals to be the best strategy as it does not involve surgical interventions, does not require hospitalization, as it is performed in day-hospital, and guarantees the right compromise between invasiveness and specificity.

However, CT-based imaging techniques expose to ionizing radiation, magnetic resonance examinations are characterized by long waiting times and the processing of peripheral blood stripes requires the use of innovative equipment available only into specialized centres.

Starting from the reported premises, this work has focused in particular on four innovative imaging methodologies that offer in each domain the advantages that will be summarized below and thus produce the case history useful to extract the information needed to implement decision support systems with very high performance levels, such as those presented in the previous paragraphs, using similar and well-established workflows.

Digital Tomosynthesis for breast cancer is an innovative method of identifying the lesions of interest with great accuracy and specificity, and, while being a technique based on ionizing radiations, it is characterized by a dose release lower than that of traditional CT. Therefore it can be assumed that in the near future it can be a valid alternative to magnetic resonance imaging, which, as is well known, does not exhibit ionizing radiation, but is less specific than tomographic techniques.

The triphasic CT technique with contrast medium for hepatocellular carcinoma detection and staging, although characterized by ionizing radiation exposures and by preliminary protocols for the administration of contrast medium that, as is well known, is nephrotoxic and has to be very carefully submitted to allergic patients, represents a novel technique, as it enables to have more observing windows thanks to its high specificity. Overall, the increasing amount of observing windows reduces the expected level of exposure to ionizing radiation during the classical period of disease monitoring.

On the other hand, the peripheral blood smear technique is absolutely not invasive, but requires the presence of instrumentation and specialized personnel that, nowadays, is not available in all the centres. Therefore, it is assumed to be a technique that can be used in the immediate future even through teleconsultation or telemedicine, which are increasing in internal medicine and hematology units.

References

[1] W. H. Organization, et al., Global health observatory data repository. 2011. number of deaths (world) by cause (2015).

[2] J. Ferlay, I. Soerjomataram, R. Dikshit, S. Eser, C. Mathers, M. Rebelo, D. M. Parkin, D. Forman, F. Bray, Cancer incidence and mortality

worldwide: sources, methods and major patterns in globocan 2012, International journal of cancer 136 (5).

[3] J. Ferlay, E. Steliarova-Foucher, J. Lortet-Tieulent, S. Rosso, J. Co- ebergh, H. Comber, D. Forman, F. Bray, Cancer incidence and mor- tality patterns in europe: estimates for 40 countries in 2012, European journal of cancer 49 (6) (2013) 1374–1403.

[4] J. T. Bushberg, The essential physics of medical imaging, Lippincott Williams & Wilkins, 2002.

[5] S. Webb, The physics of medical imaging, CRC Press, 1988.

[6] C. M. Tempany, K. H. Zou, S. G. Silverman, D. L. Brown, A. B. Kurtz, B. J. McNeil, Staging of advanced ovarian cancer: comparison of imaging modalitiesâĂŤreport from the radiological diagnostic oncology group, Radiology 215 (3) (2000) 761–767.

[7] S. G. Orel, M. D. Schnall, Mr imaging of the breast for the detection, diagnosis, and staging of breast cancer, Radiology 220 (1) (2001) 13–30.

[8] V. Kut, W. Spies, S. Spies, W. Gooding, A. Argiris, Staging and mon- itoring of small cell lung cancer using [18f] fluoro-2-deoxy-d-glucose- positron emission tomography (fdg-pet)., American journal of clinical oncology 30 (1) (2007) 45–50.

[9] S. Astley, F. J. Gilbert, Computer-aided detection in mammography, Clinical radiology 59 (5) (2004) 390–399.

[10] M. Sonka, J. M. Fitzpatrick, Handbook of medical imaging(volume 2, medical image processing and analysis), SPIE- The international society for optical engineering, 2000.

[11] A. Wagner, H. Mahrholdt, T. A. Holly, M. D. Elliott, M. Regen- fus, M. Parker, F. J. Klocke, R. O. Bonow, R. J. Kim, R. M. Judd, Contrast-enhanced mri and routine single photon emission computed tomography (spect) perfusion imaging for detection of subendocardial myocardial infarcts: an imaging study, The Lancet 361 (9355) (2003) 374–379.

[12] K. Doi, Diagnostic imaging over the last 50 years: research and development in medical imaging science and technology, Physics in Medicine & Biology 51 (13) (2006) R5.

[13] G. Muehllehner, J. S. Karp, Positron emission tomography, Physics in medicine and biology 51 (13) (2006) R117.

[14] J. Hsieh, et al., Computed tomography: principles, design, artifacts, and recent advances, SPIE Bellingham, WA, 2009.

[15] S. Rahnamayan, Z. Mohamad, Tissue segmentation in medical images based on image processing chain optimization, in: International Workshop on Real Time Measurement, Instrumentation and Control, Toronto, 2010, pp. 1–9.

[16] V. Bevilacqua, A. Aulenta, E. Carioggia, G. Mastronardi, F. Menolascina, G. Simeone, A. Paradiso, A. Scarpa, D. Taurino, Metallic artifacts removal in breast CT images for treatment planning in radiotherapy by means of supervised and unsupervised neural network algorithms, in: D. Huang, L. Heutte, M. Loog (Eds.), Advanced Intelligent Computing Theories and Applications. With Aspects of Theoretical and Methodological Issues, Third International Conference on Intelligent Computing, ICIC 2007, Qingdao, China, August 21-24, 2007, Proceedings, Vol. 4681 of Lecture Notes in Computer Science, Springer, 2007, pp. 1355–1363. doi:10.1007/978-3-540-74171-8_138.

[17] M. O. Al-Hatmi, J. H. Yousif, A review of image enhancement systems and a case study of salt &pepper noise removing, International Journal of Computation and Applied Sciences IJOCAAS 3 (2) (2017) 217–223.

[18] B. Suneetha, A. JhansiRani, A survey on image processing techniques for brain tumor detection using magnetic resonance imaging, in: Innovations in Green Energy and Healthcare Technologies (IGEHT), 2017 International Conference on, IEEE, 2017, pp. 1–6.

[19] G. Niranjana, M. Ponnavaikko, A review on image processing methods in detecting lung cancer using ct images, in: Technical Advancements in Computers and Communications (ICTACC), 2017 International Conference on, IEEE, 2017, pp. 18–25.

[20] K.-S. Fu, J. Mui, A survey on image segmentation, Pattern recognition 13 (1) (1981) 3–16.

[21] H. Zhang, J. E. Fritts, S. A. Goldman, Image segmentation evaluation: A survey of unsupervised methods, computer vision and image understanding 110 (2) (2008) 260–280.

[22] N. Kumar, Thresholding in salient object detection: a survey, Multimedia Tools and Applications (2017) 1–32.

[23] V. Bevilacqua, A. Piazzolla, P. Stofella, Atlas-based segmentation of organs at risk in radiotherapy in head mris by means of a novel active contour framework, in: D. Huang, X. Zhang, C. A. R. García, L. Zhang (Eds.), Advanced Intelligent Computing Theories and Applications. With Aspects of Artificial Intelligence, 6th International Conference on Intelligent Computing, ICIC 2010, Changsha, China, August 18-21, 2010. Proceedings, Vol. 6216 of Lecture Notes in Computer Science, Springer, 2010, pp. 350–359. doi:10.1007/978-3-642-14932-0_44.

[24] Y. LeCun, Y. Bengio, G. Hinton, Deep learning, Nature 521 (7553) (2015) 436–444.

[25] V. Bevilacqua, N. Pietroleonardo, V. Triggiani, A. Brunetti, A. D. Palma, M. Rossini, L. Gesualdo, An innovative neural network framework to classify blood vessels and tubules based on haralick features evaluated in histological images of kidney biopsy, Neurocomputing 228 (2017) 143–153. doi:10.1016/j.neucom.2016.09.091.

[26] Y. Kimori, Mathematical morphology-based approach to the enhancement of morphological features in medical images, Journal of clinical bioinformatics 1 (1) (2011) 33.

[27] B. Sahiner, H.-P. Chan, N. Petrick, M. A. Helvie, L. M. Hadjiiski, Improvement of mammographic mass characterization using spiculation measures and morphological features, Medical Physics 28 (7) (2001) 1455–1465.

[28] W.-J. Wu, W. K. Moon, Ultrasound breast tumor image computer-aided diagnosis with texture and morphological features, Academic radiology 15 (7) (2008) 873–880.

[29] R. M. Haralick, K. Shanmugam, et al., Textural features for image classification, IEEE Transactions on systems, man, and cybernetics (6) (1973) 610–621.

[30] T. Ojala, M. Pietikainen, T. Maenpaa, Multiresolution gray-scale and rotation invariant texture classification with local binary patterns, IEEE Transactions on pattern analysis and machine intelligence 24 (7) (2002) 971–987.

[31] N. A. Hamilton, R. S. Pantelic, K. Hanson, R. D. Teasdale, Fast automated cell phenotype image classification, BMC bioinformatics 8 (1) (2007) 110.

[32] H. Bay, T. Tuytelaars, L. Van Gool, Surf: Speeded up robust features, Computer vision–ECCV 2006 (2006) 404–417.

[33] R. M. Rangayyan, Biomedical image analysis, CRC press, 2004.

[34] V. Bevilacqua, M. Triggiani, M. Dimatteo, G. Bellantuono, A. Brunetti, L. Carnimeo, F. Marino, M. Telegrafo, M. Moschetta, Computer assisted detection of breast lesions in magnetic resonance images, in: D. Huang, V. Bevilacqua, P. Premaratne (Eds.), Intelligent Computing Theories and Application - 12th International Conference, ICIC 2016, Lanzhou, China, August 2-5, 2016, Proceedings, Part I, Vol. 9771 of Lecture Notes in Computer Science, Springer, 2016, pp. 306–316. doi:10.1007/978-3-319-42291-6_30.

[35] V. Bevilacqua, A. Brunetti, M. Triggiani, D. Magaletti, M. Telegrafo, M. Moschetta, An optimized feed-forward artificial neural network topology to support radiologists in breast lesions classification, in: T. Friedrich, F. Neumann, A. M. Sutton (Eds.), Genetic and Evolutionary Computation Conference, GECCO 2016, Denver, CO, USA, July 20-24, 2016, Companion Material Proceedings, ACM, 2016, pp. 1385–1392. doi:10.1145/2908961.2931733.

[36] S. Sharma, P. Khanna, Computer-aided diagnosis of malignant mammograms using zernike moments and svm, Journal of Digital Imaging 28 (1) (2015) 77–90. doi:10.1007/s10278-014-9719-7.

[37] J. Dheeba, N. A. Singh, S. T. Selvi, Computer-aided detection of breast cancer on mammograms: A swarm intelligence optimized wavelet neural network approach, Journal of biomedical informatics 49 (2014) 45–52.

[38] I. Saritas, Prediction of breast cancer using artificial neural networks, Journal of Medical Systems 36 (5) (2012) 2901–2907.

[39] V. Bevilacqua, P. Pannarale, M. Abbrescia, C. Cava, A. Paradiso, S. Tommasi, Comparison of data-merging methods with svm attribute selection and classification in breast cancer gene expression, BMC bioinformatics 13 (7) (2012) S9.

[40] H.-L. Chen, B. Yang, J. Liu, D.-Y. Liu, A support vector machine classifier with rough set-based feature selection for breast cancer diagnosis, Expert Systems with Applications 38 (7) (2011) 9014–9022.

[41] J. Jiang, P. Trundle, J. Ren, Medical image analysis with artificial neural networks, Computerized Medical Imaging and Graphics 34 (8) (2010) 617–631.

[42] R. Janghel, A. Shukla, R. Tiwari, R. Kala, Breast cancer diagnosis using artificial neural network models, in: Information Sciences and Interaction Sciences (ICIS), 2010 3rd International Conference on, IEEE, 2010, pp. 89–94.

[43] D. Newell, K. Nie, J.-H. Chen, C.-C. Hsu, H. J. Yu, O. Nalcioglu, M.-Y. Su, Selection of diagnostic features on breast mri to differentiate between malignant and benign lesions using computer-aided diagnosis: differences in lesions presenting as mass and non-mass-like enhancement, European Radiology 20 (4) (2010) 771–781. doi:10.1007/s00330-009-1616-y.

[44] Y. Rejani, S. T. Selvi, Early detection of breast cancer using svm classifier technique, arXiv preprint arXiv:0912.2314.

[45] M. F. Akay, Support vector machines combined with feature selection for breast cancer diagnosis, Expert systems with applications 36 (2) (2009) 3240–3247.

[46] V. Bevilacqua, G. Mastronardi, F. Menolascina, P. Pannarale, A. Pedone, A novel multi-objective genetic algorithm approach to artificial neural network topology optimisation: The breast cancer classification problem, in: Proceedings of the International Joint Conference on Neural Networks, IJCNN 2006, part of the IEEE World Congress on Computational Intelligence, WCCI 2006, Vancouver, BC, Canada, 16-21 July 2006, IEEE, 2006, pp. 1958–1965. doi:10.1109/IJCNN.2006.246940.

[47] H. A. Abbass, An evolutionary artificial neural networks approach for breast cancer diagnosis, Artificial intelligence in Medicine 25 (3) (2002) 265–281.

[48] D.-S. Huang, Systematic theory of neural networks for pattern recognition, Publishing House of Electronic Industry of China, Beijing 201.

[49] D.-s. Huang, Radial basis probabilistic neural networks: Model and application, International Journal of Pattern Recognition and Artificial Intelligence 13 (07) (1999) 1083–1101.

[50] D.-S. Huang, J.-X. Du, A constructive hybrid structure optimization methodology for radial basis probabilistic neural networks, IEEE Transactions on Neural Networks 19 (12) (2008) 2099–2115.

[51] I. Basheer, M. Hajmeer, Artificial neural networks: fundamentals, computing, design, and application, Journal of microbiological methods 43 (1) (2000) 3–31.

[52] E. B. Baum, D. Haussler, What size net gives valid generalization?, in: Advances in neural information processing systems, 1989, pp. 81–90.

[53] F. U. Dowla, L. L. Rogers, Solving problems in environmental engineering and geosciences with artificial neural networks, Mit Press, 1995.

[54] S. Haykin, N. Network, A comprehensive foundation, Neural Networks 2 (2004) (2004) 41.

[55] T. Masters, Practical neural network recipes in C++, Morgan Kaufmann, 1993.

[56] C. G. Looney, Advances in feedforward neural networks: demystifying knowledge acquiring black boxes, IEEE Transactions on Knowledge and Data Engineering 8 (2) (1996) 211–226.

[57] K. Swingler, Applying neural networks: a practical guide, Morgan Kaufmann, 1996.

[58] S. Arlot, A. Celisse, et al., A survey of cross-validation procedures for model selection, Statistics surveys 4 (2010) 40–79.

[59] L. B. Lusted, Decision-making studies in patient management, New England Journal of Medicine 284 (8) (1971) 416–424.

[60] D. J. Goodenough, K. Rossmann, L. B. Lusted, Radiographic applications of receiver operating characteristic (roc) curves, Radiology 110 (1) (1974) 89–95.

[61] C. E. Metz, Basic principles of roc analysis, in: Seminars in nuclear medicine, Vol. 8, Elsevier, 1978, pp. 283–298.

[62] J. A. Hanley, B. J. McNeil, The meaning and use of the area under a receiver operating characteristic (roc) curve., Radiology 143 (1) (1982) 29–36.

[63] J. A. Nevin, Signal detection theory and operant behavior: A review of david m. green and john a. swets' signal detection theory and psychophysics., Journal of the Experimental Analysis of Behavior 12 (3) (1969) 475–480.

[64] M. Oquab, L. Bottou, I. Laptev, J. Sivic, Learning and transferring mid-level image representations using convolutional neural networks, in: The IEEE Conference on Computer Vision and Pattern Recognition (CVPR), 2014.

[65] A. Krizhevsky, I. Sutskever, G. E. Hinton, Imagenet classification with deep convolutional neural networks, in: Advances in neural information processing systems, 2012, pp. 1097–1105.

[66] A. Vedaldi, K. Lenc, Matconvnet: Convolutional neural networks for matlab, in: Proceedings of the 23rd ACM international conference on Multimedia, ACM, 2015, pp. 689–692.

[67] P. Tokarczyk, J. D. Wegner, S. Walk, K. Schindler, Beyond hand-crafted features in remote sensing, ISPRS Annals of Photogrammetry, Remote Sensing and Spatial Information Sciences (1) (2013) 35–40.

[68] H. Lee, R. Grosse, R. Ranganath, A. Y. Ng, Unsupervised learning of hierarchical representations with convolutional deep belief networks, Communications of the ACM 54 (10) (2011) 95–103.

[69] D. A. Winkler, T. C. Le, Performance of deep and shallow neural networks, the universal approximation theorem, activity cliffs, and qsar, Molecular informatics 36 (1-2).

[70] J. Schmidhuber, Deep learning in neural networks: An overview, Neural networks 61 (2015) 85–117.

[71] M. Bianchini, F. Scarselli, On the complexity of neural network classifiers: A comparison between shallow and deep architectures, IEEE transactions on neural networks and learning systems 25 (8) (2014) 1553–1565.

[72] A. Ali, S. M. Shamsuddin, A. L. Ralescu, Classification with class imbalance problem: a review, Int. J. Advance Soft Compu. Appl 7 (3).

[73] M. A. Nielsen, Neural networks and deep learning (2015).

[74] P. Benardos, G.-C. Vosniakos, Optimizing feedforward artificial neural network architecture, Engineering Applications of Artificial Intelligence 20 (3) (2007) 365–382.

[75] S. Albarqouni, C. Baur, F. Achilles, V. Belagiannis, S. Demirci, N. Navab, Aggnet: deep learning from crowds for mitosis detection in breast cancer histology images, IEEE transactions on medical imaging 35 (5) (2016) 1313–1321.

[76] G. Apou, N. S. Schaadt, B. Naegel, G. Forestier, R. Schönmeyer, F. Feuerhake, C. Wemmert, A. Grote, Detection of lobular structures in normal breast tissue, Computers in biology and medicine 74 (2016) 91–102.

[77] J.-Z. Cheng, D. Ni, Y.-H. Chou, J. Qin, C.-M. Tiu, Y.-C. Chang, C.-S. Huang, D. Shen, C.-M. Chen, Computer-aided diagnosis with deep

learning architecture: applications to breast lesions in us images and pulmonary nodules in ct scans, Scientific reports 6 (2016) 24454.

[78] D. C. Cireşan, A. Giusti, L. M. Gambardella, J. Schmidhuber, Mitosis detection in breast cancer histology images with deep neural networks, in: International Conference on Medical Image Computing and Computer-assisted Intervention, Springer, 2013, pp. 411–418.

[79] M. U. Dalmış, G. Litjens, K. Holland, A. Setio, R. Mann, N. Karssemeijer, A. Gubern-Mérida, Using deep learning to segment breast and fibroglandular tissue in mri volumes, Medical physics 44 (2) (2017) 533–546.

[80] N. Dhungel, G. Carneiro, A. P. Bradley, The automated learning of deep features for breast mass classification from mammograms, in: International Conference on Medical Image Computing and Computer-Assisted Intervention, Springer, 2016, pp. 106–114.

[81] A. Dubrovina, P. Kisilev, B. Ginsburg, S. Hashoul, R. Kimmel, Computational mammography using deep neural networks, Computer Methods in Biomechanics and Biomedical Engineering: Imaging & Visualization (2016) 1–5.

[82] P. Fonseca, J. Mendoza, J. Wainer, J. Ferrer, J. Pinto, J. Guerrero, B. Castaneda, Automatic breast density classification using a convolutional neural network architecture search procedure, in: Proc. of SPIE Vol, Vol. 9414, 2015, pp. 941428–1.

[83] S. V. Fotin, Y. Yin, H. Haldankar, J. W. Hoffmeister, S. Periaswamy, Detection of soft tissue densies from digital breast tomosynthesis: comparison of conventional and deep learning approaches, in: Proc. SPIE, Vol. 9785, 2016.

[84] B. Q. Huynh, H. Li, M. L. Giger, Digital mammographic tumor classification using transfer learning from deep convolutional neural networks, Journal of Medical Imaging 3 (3) (2016) 034501–034501.

[85] A. R. Jamieson, K. Drukker, M. L. Giger, Breast image feature learning with adaptive deconvolutional networks, SPIE Medical Imaging, Strony 2012 (2012) 831506–831506.

[86] T. Kooi, G. Litjens, B. van Ginneken, A. Gubern-Mérida, C. I. Sánchez, R. Mann, A. den Heeten, N. Karssemeijer, Large scale deep learning for computer aided detection of mammographic lesions, Medical image analysis 35 (2017) 303–312.

[87] T. Kooi, B. Ginneken, N. Karssemeijer, A. Heeten, Discriminating solitary cysts from soft tissue lesions in mammography using a pretrained deep convolutional neural network, Medical physics 44 (3) (2017) 1017–1027.

[88] K. Paeng, S. Hwang, S. Park, M. Kim, A unified framework for tumor proliferation score prediction in breast histopathology, in: Deep Learning in Medical Image Analysis and Multimodal Learning for Clinical Decision Support, Springer, 2017, pp. 231–239.

[89] R. K. Samala, H.-P. Chan, L. Hadjiiski, M. A. Helvie, J. Wei, K. Cha, Mass detection in digital breast tomosynthesis: Deep convolutional neural network with transfer learning from mammography, Medical physics 43 (12) (2016) 6654–6666.

[90] W. Sun, T.-L. B. Tseng, J. Zhang, W. Qian, Enhancing deep convolutional neural network scheme for breast cancer diagnosis with unlabeled data, Computerized Medical Imaging and Graphics 57 (2017) 4–9.

[91] D. Wang, A. Khosla, R. Gargeya, H. Irshad, A. H. Beck, Deep learning for identifying metastatic breast cancer, arXiv preprint arXiv:1606.05718.

[92] J. Xu, L. Xiang, Q. Liu, H. Gilmore, J. Wu, J. Tang, A. Madabhushi, Stacked sparse autoencoder (ssae) for nuclei detection on breast cancer histopathology images, IEEE transactions on medical imaging 35 (1) (2016) 119–130.

[93] Q. Zhang, Y. Xiao, W. Dai, J. Suo, C. Wang, J. Shi, H. Zheng, Deep learning based classification of breast tumors with shear-wave elastography, Ultrasonics 72 (2016) 150–157.

[94] S. V. Stehman, Selecting and interpreting measures of thematic classification accuracy, Remote sensing of Environment 62 (1) (1997) 77–89.

[95] T. Fawcett, An introduction to roc analysis, Pattern recognibion letters 27 (8) (2006) 861–874.

[96] D. M. Powers, Evaluation: from precision, recall and f-measure to roc, informedness, markedness and correlation.

[97] A. Vestito, F. F. Mangieri, G. Gatta, M. Moschetta, B. Turi, A. Ancona, Breast carcinoma in elderly women. our experience, Il giornale di chirurgia 32 (1) (2011) 411–416.

[98] D. Saslow, C. Boetes, W. Burke, S. Harms, M. O. Leach, C. D. Lehman, E. Morris, E. Pisano, M. Schnall, S. Sener, et al., American cancer society guidelines for breast screening with mri as an adjunct to mammography, CA: a cancer journal for clinicians 57 (2) (2007) 75–89.

[99] R. K. Samala, H.-P. Chan, L. Hadjiiski, K. Cha, M. A. Helvie, Deep-learning convolution neural network for computer-aided detection of microcalcifications in digital breast tomosynthesis, SPIE medical imaging. International Society for Optics and Photonics (2016) 97850Y–97850Y.

[100] M. Kallenberg, K. Petersen, M. Nielsen, A. Y. Ng, P. Diao, C. Igel, C. M. Vachon, K. Holland, R. R. Winkel, N. Karssemeijer, et al., Unsupervised deep learning applied to breast density segmentation and mammographic risk scoring, IEEE transactions on medical imaging 35 (5) (2016) 1322–1331.

[101] N. V. Chawla, K. W. Bowyer, L. O. Hall, W. P. Kegelmeyer, Smote: synthetic minority over-sampling technique, Journal of artificial intelligence research 16 (2002) 321–357.

[102] E. D. Pisano, C. A. Parham, Digital mammography, sestamibi breast scintigraphy, and positron emission tomography breast imaging, Radiologic Clinics of North America 38 (4) (2000) 861–869.

[103] H.-P. Chan, J. Wei, B. Sahiner, E. A. Rafferty, T. Wu, M. A. Roubidoux, R. H. Moore, D. B. Kopans, L. M. Hadjiiski, M. A. Helvie, Computer-aided detection system for breast masses on digital tomosynthesis mammograms: preliminary experience, Radiology 237 (3) (2005) 1075–1080.

[104] J. M. Boone, A. L. Kwan, K. Yang, G. W. Burkett, K. K. Lindfors, T. R. Nelson, Computed tomography for imaging the breast, Journal of mammary gland biology and neoplasia 11 (2) (2006) 103–111.

[105] T. Wu, J. Zhang, R. Moore, E. Rafferty, D. Kopans, W. Meleis, D. Kaeli, Digital tomosynthesis mammography using a parallel maximum-likelihood reconstruction method, in: Proc. SPIE, Vol. 5368, 2004, pp. 0277–786X.

[106] K. E. Korhonen, S. P. Weinstein, E. S. McDonald, E. F. Conant, Strategies to increase cancer detection: Review of true-positive and false-negative results at digital breast tomosynthesis screening, Radio-Graphics 36 (7) (2016) 1954–1965.

[107] V. Bevilacqua, D. Altini, M. Bruni, M. Riezzo, A. Brunetti, C. Locon-sole, A. Guerriero, G. F. Trotta, R. Fasano, M. D. Pirchio, C. Tartaglia, E. Ventrella, M. Telegrafo, M. Moschetta, A supervised breast lesion images classification from tomosynthesis technique, in: D. Huang, K. Jo, J. C. Figueroa-García (Eds.), Intelligent Computing Theories and Application - 13th International Conference, ICIC 2017, Liver-pool, UK, August 7-10, 2017, Proceedings, Part II, Vol. 10362 of Lecture Notes in Computer Science, Springer, 2017, pp. 483–489. doi:10.1007/978-3-319-63312-1_42.

[108] L.-K. Soh, C. Tsatsoulis, Texture analysis of sar sea ice imagery using gray level co-occurrence matrices, IEEE Transactions on geoscience and remote sensing 37 (2) (1999) 780–795.

[109] D. A. Clausi, An analysis of co-occurrence texture statistics as a func-tion of grey level quantization, Canadian Journal of remote sensing 28 (1) (2002) 45–62.

[110] C. Szegedy, W. Liu, Y. Jia, P. Sermanet, S. Reed, D. Anguelov, D. Er-han, V. Vanhoucke, A. Rabinovich, Going deeper with convolutions, in: Proceedings of the IEEE conference on computer vision and pat-tern recognition, 2015, pp. 1–9.

[111] K. He, X. Zhang, S. Ren, J. Sun, Deep residual learning for image recognition, in: Proceedings of the IEEE conference on computer vision and pattern recognition, 2016, pp. 770–778.

[112] Y. LeCun, L. Bottou, Y. Bengio, P. Haffner, Gradient-based learning applied to document recognition, Proceedings of the IEEE 86 (11) (1998) 2278–2324.

[113] K. Simonyan, A. Zisserman, Very deep convolutional networks for large-scale image recognition, arXiv preprint arXiv:1409.1556.

[114] K. Chatfield, K. Simonyan, A. Vedaldi, A. Zisserman, Return of the devil in the details: Delving deep into convolutional nets, arXiv preprint arXiv:1405.3531.

[115] P. Sermanet, D. Eigen, X. Zhang, M. Mathieu, R. Fergus, Y. LeCun, Overfeat: Integrated recognition, localization and detection using convolutional networks, arXiv preprint arXiv:1312.6229.

[116] M. D. Zeiler, R. Fergus, Visualizing and understanding convolutional networks, in: European conference on computer vision, Springer, 2014, pp. 818–833.

[117] C. J. Burges, A tutorial on support vector machines for pattern recognition, Data mining and knowledge discovery 2 (2) (1998) 121–167.

[118] K. Beyer, J. Goldstein, R. Ramakrishnan, U. Shaft, When is âĂIJnearest neighborâĂİ meaningful?, in: International conference on database theory, Springer, 1999, pp. 217–235.

[119] P. Domingos, M. Pazzani, On the optimality of the simple bayesian classifier under zero-one loss, Machine learning 29 (2) (1997) 103–130.

[120] H. Dahan, S. Cohen, L. Rokach, O. Maimon, Proactive data mining with decision trees, Springer Science & Business Media, 2014.

[121] R. A. Fisher, The use of multiple measurements in taxonomic problems, Annals of human genetics 7 (2) (1936) 179–188.

[122] B. Li, C.-H. Zheng, D.-S. Huang, Locally linear discriminant embedding: An efficient method for face recognition, Pattern Recognition 41 (12) (2008) 3813–3821.

[123] P. F. Christ, F. Ettlinger, F. Grün, M. E. A. Elshaera, J. Lipkova, S. Schlecht, F. Ahmaddy, S. Tatavarty, M. Bickel, P. Bilic,

et al., Automatic liver and tumor segmentation of ct and mri volumes using cascaded fully convolutional neural networks, arXiv preprint arXiv:1702.05970.

[124] X. Han, Automatic liver lesion segmentation using a deep convolutional neural network method, arXiv preprint arXiv:1704.07239.

[125] M. Fatima, M. Pasha, Survey of machine learning algorithms for disease diagnostic, Journal of Intelligent Learning Systems and Applications 9 (01) (2017) 1.

[126] S. Vijayarani, S. Dhayanand, Liver disease prediction using svm and naïve bayes algorithms, International Journal of Science, Engineering and Technology Research (IJSETR) 4 (4) (2015) 816–820.

[127] A. Gulia, R. Vohra, P. Rani, Liver patient classification using intelligent techniques, International Journal of Computer Science and Information Technologies 5 (4) (2014) 5110–5115.

[128] F. M. Ba-Alwi, H. M. Hintaya, Comparative study for analysis the prognostic in hepatitis data: data mining approach, spinal cord 11 (2013) 12.

[129] B. Karlik, Hepatitis disease diagnosis using backpropagation and the naive bayes classifiers, IBU Journal of Science and Technology 1 (1).

[130] G. Sathyadevi, Application of cart algorithm in hepatitis disease diagnosis, in: Recent Trends in Information Technology (ICRTIT), 2011 International Conference on, IEEE, 2011, pp. 1283–1287.

[131] P. Rajeswari, G. S. Reena, Analysis of liver disorder using data mining algorithm, Global journal of computer science and technology 10 (14).

[132] R. Vivanti, A. Szeskin, N. Lev-Cohain, J. Sosna, L. Joskowicz, Automatic detection of new tumors and tumor burden evaluation in longitudinal liver ct scan studies, International Journal of Computer Assisted Radiology and Surgery 12 (11) (2017) 1945–1957.

[133] Y. Yuan, Hierarchical convolutional-deconvolutional neural networks for automatic liver and tumor segmentation, arXiv preprint arXiv:1710.04540.

[134] A. Ben-Cohen, I. Diamant, E. Klang, M. Amitai, H. Greenspan, Fully convolutional network for liver segmentation and lesions detection, in: International Workshop on Large-Scale Annotation of Biomedical Data and Expert Label Synthesis, Springer, 2016, pp. 77–85.

[135] W. Li, F. Jia, Q. Hu, Automatic segmentation of liver tumor in ct images with deep convolutional neural networks, Journal of Computer and Communications 3 (11) (2015) 146.

[136] S. Kumar, D. Devapal, Survey on recent cad system for liver disease diagnosis, in: Control, Instrumentation, Communication and Computational Technologies (ICCICCT), 2014 International Conference on, IEEE, 2014, pp. 763–766.

[137] A. Adcock, D. Rubin, G. Carlsson, Classification of hepatic lesions using the matching metric, Computer vision and image understanding 121 (2014) 36–42.

[138] S. Kumar, R. Moni, J. Rajeesh, Automatic liver and lesion segmentation: a primary step in diagnosis of liver diseases, Signal, Image and Video Processing (2013) 1–10.

[139] P. Dankerl, A. Cavallaro, A. Tsymbal, M. J. Costa, M. Suehling, R. Janka, M. Uder, M. Hammon, A retrieval-based computer-aided diagnosis system for the characterization of liver lesions in ct scans, Academic radiology 20 (12) (2013) 1526–1534.

[140] J. Vincey, M. Jeba, Computer aided diagnosis for liver cancer feature extraction, The International Journal of Engineering and Science (IJES) 2 (11) (2013) 27–30.

[141] D. Duda, M. Krętowski, J. Bézy-Wendling, Computer-aided diagnosis of liver tumors based on multi-image texture analysis of contrast-enhanced ct. selection of the most appropriate texture features, Studies in Logic, Grammar and Rhetoric 35 (1) (2013) 49–70.

[142] Y.-W. Chen, J. Luo, C. Dong, X. Han, T. Tateyama, A. Furukawa, S. Kanasaki, Computer-aided diagnosis and quantification of cirrhotic livers based on morphological analysis and machine learning, Computational and mathematical methods in medicine 2013.

[143] A. Thakre, A. Dhenge, Ct liver image diagnosis classification system, International Journal of Advanced Research in Computer and Communication Engineering 2 (1).

[144] P. Sharma, S. Malik, S. Sehgal, J. Pruthi, Computer aided diagnosis based on medical image processing and artificial intelligence methods, International Journal of Information and Computation Technology 3 (9) (2013) 887–92.

[145] S. Gunasundari, M. S. Ananthi, Comparison and evaluation of methods for liver tumor classification from ct datasets, International journal of computer applications 39 (18) (2012) 46–51.

[146] R. S. Hameed, S. Kumar, Assessment of neural network based classifiers to diagnose focal liver lesions using ct images, Procedia Engineering 38 (2012) 4048–4056.

[147] Ö. Kayaalti, B. H. Aksebzeci, I. Ö. Karahan, K. Deniz, M. Öztürk, B. Yilmaz, S. Kara, M. H. Asyali, Staging of the liver fibrosis from ct images using texture features, in: Health Informatics and Bioinformatics (HIBIT), 2012 7th International Symposium on, IEEE, 2012, pp. 47–52.

[148] S. Kumar, R. Moni, Diagnosis of liver tumor from ct images using fast discrete curvelet transform, IJCA Special Issue on Computer Aided Soft Computing Techniques for Imaging and Biomedical Applications (CASCT) (2010) 48–57.

[149] S. G. Mougiakakou, I. Valavanis, K. Nikita, A. Nikita, D. Kelekis, Characterization of ct liver lesions based on texture features and a multiple neural network classification scheme, in: Engineering in Medicine and Biology Society, 2003. Proceedings of the 25th Annual International Conference of the IEEE, Vol. 2, IEEE, 2003, pp. 1287–1290.

[150] A. Cucchetti, F. Piscaglia, A. D. Grigioni, M. Ravaioli, M. Cescon, M. Zanello, G. L. Grazi, R. Golfieri, W. F. Grigioni, A. D. Pinna, Preoperative prediction of hepatocellular carcinoma tumour grade and micro-vascular invasion by means of artificial neural network: a pilot study, Journal of hepatology 52 (6) (2010) 880–888.

[151] K. Mala, V. Sadasivam, S. Alagappan, Neural network based texture analysis of liver tumor from computed tomography images, International Journal of Biological and Medical Sciences 21 (2007) 33–41.

[152] Y.-L. Huang, J.-H. Chen, W.-C. Shen, Diagnosis of hepatic tumors with texture analysis in nonenhanced computed tomography images, Academic radiology 13 (6) (2006) 713–720.

[153] V. Bevilacqua, A. Brunetti, G. F. Trotta, G. Dimauro, K. Elez, V. Alberotanza, A. Scardapane, A novel approach for hepatocellular carcinoma detection and classification based on triphasic ct protocol, in: Evolutionary Computation (CEC), 2017 IEEE Congress on, IEEE, 2017, pp. 1856–1863.

[154] M. Memeo, A. I. Stabile, A. Scardapane, P. Suppressa, A. Cirulli, C. Sabba, A. Rotondo, G. Angelelli, Hereditary haemorrhagic telangiectasia: study of hepatic vascular alterations with multi-detector row helical ct and reconstruction programs., La Radiologia Medica 109 (1-2) (2005) 125–138.

[155] I. A. Stabile, P. Pedote, A. Scardapane, M. Memeo, A. Rotondo, G. Angelelli, Preoperative staging of gastric carcinoma with multidetector spiral ct., La Radiologia medica 106 (5-6) (2003) 467.

[156] S. Kullback, R. A. Leibler, On information and sufficiency, The annals of mathematical statistics 22 (1) (1951) 79–86.

[157] H. A. Edmondson, P. E. Steiner, Primary carcinoma of the liver. a study of 100 cases among 48,900 necropsies, Cancer 7 (3) (1954) 462–503.

[158] V. Bevilacqua, A. Brunetti, G. F. Trotta, L. Carnimeo, F. Marino, V. Alberotanza, A. Scardapane, A deep learning approach for hepatocellular carcinoma grading, IJCVIP 7 (2) (2017) 1–18. doi:10.4018/IJCVIP.2017040101.

[159] C. Szegedy, V. Vanhoucke, S. Ioffe, J. Shlens, Z. Wojna, Rethinking the inception architecture for computer vision, in: Proceedings of the IEEE Conference on Computer Vision and Pattern Recognition, 2016, pp. 2818–2826.

[160] S. U. Akram, J. Kannala, L. Eklund, J. Heikkilä, Cell segmentation proposal network for microscopy image analysis, in: International Workshop on Large-Scale Annotation of Biomedical Data and Expert Label Synthesis, Springer, 2016, pp. 21–29.

[161] A. Ferrari, S. Lombardi, A. Signoroni, Bacterial colony counting by convolutional neural networks, in: Engineering in Medicine and Biology Society (EMBC), 2015 37th Annual International Conference of the IEEE, IEEE, 2015, pp. 7458–7461.

[162] Z. Gao, L. Wang, L. Zhou, J. Zhang, Hep-2 cell image classification with deep convolutional neural networks, IEEE journal of biomedical and health informatics 21 (2) (2017) 416–428.

[163] M. N. Kashif, S. E. A. Raza, K. Sirinukunwattana, M. Arif, N. Rajpoot, Handcrafted features with convolutional neural networks for detection of tumor cells in histology images, in: Biomedical Imaging (ISBI), 2016 IEEE 13th International Symposium on, IEEE, 2016, pp. 1029–1032.

[164] H. T. H. Phan, A. Kumar, J. Kim, D. Feng, Transfer learning of a convolutional neural network for hep-2 cell image classification, in: Biomedical Imaging (ISBI), 2016 IEEE 13th International Symposium on, IEEE, 2016, pp. 1208–1211.

[165] A. Shkolyar, A. Gefen, D. Benayahu, H. Greenspan, Automatic detection of cell divisions (mitosis) in live-imaging microscopy images using convolutional neural networks, in: Engineering in Medicine and Biology Society (EMBC), 2015 37th Annual International Conference of the IEEE, IEEE, 2015, pp. 743–746.

[166] J. Zhao, M. Zhang, Z. Zhou, J. Chu, F. Cao, Automatic detection and classification of leukocytes using convolutional neural networks, Medical & biological engineering & computing 55 (8) (2017) 1287–1301.

[167] C. Dong, C. C. Loy, K. He, X. Tang, Learning a deep convolutional network for image super-resolution, in: European Conference on Computer Vision, Springer, 2014, pp. 184–199.

[168] C. Dong, C. C. Loy, K. He, X. Tang, Image super-resolution using deep convolutional networks, IEEE transactions on pattern analysis and machine intelligence 38 (2) (2016) 295–307.

[169] M. Habibzadeh, A. Krzyżak, T. Fevens, Analysis of white blood cell differential counts using dual-tree complex wavelet transform and support vector machine classifier, Computer Vision and Graphics (2012) 414–422.

[170] V. Bevilacqua, D. Buongiorno, P. Carlucci, F. Giglio, G. Tattoli, A. Guarini, N. Sgherza, G. D. Tullio, C. Minoia, A. Scattone, G. Simone, F. Girardi, A. Zito, L. Gesualdo, A supervised CAD to support telemedicine in hematology, in: 2015 International Joint Conference on Neural Networks, IJCNN 2015, Killarney, Ireland, July 12-17, 2015, IEEE, 2015, pp. 1–7. doi:10.1109/IJCNN.2015.7280464.

[171] P. Hiremath, P. Bannigidad, S. Geeta, Automated identification and classification of white blood cells (leukocytes) in digital microscopic images, IJCA special issue on âĂIJrecent trends in image processing and pattern recognitionâĂİ RTIPPR (2010) 59–63.

[172] V. Piuri, F. Scotti, Morphological classification of blood leucocytes by microscope images, in: Computational Intelligence for Measurement Systems and Applications, 2004. CIMSA. 2004 IEEE International Conference on, IEEE, 2004, pp. 103–108.

[173] M. Alagappan, B. BanuRekha, R. Arun, M. Kalaikamal, S. Muthukrishnan, C. S. Ganesh, S. Sathishkumar, Extreme learning machine (elm) based automated identification and classification of white blood cells, in: International Conference on Mathematical Modeling and Applied Soft Computing, pp. 846–852.

[174] A. Mathur, A. S. Tripathi, M. Kuse, Scalable system for classification of white blood cells from leishman stained blood stain images, Journal of pathology informatics 4 (Suppl).

[175] V. Bevilacqua, A. Brunetti, G. F. Trotta, D. De Marco, M. G. Quercia, D. Buongiorno, F. Girardi, A. Guarini, A novel deep learning approach in haematology for classification of leucocytes, in: Smart Innovation, Systems and Technologies, Springer, 2018, to appear in.